INTERNATIONAL JOURNAL FOR NUMERICAL METHODS IN FLUIDS, VOL. 25, 1421–1454 (1997)

A HIGH-ORDER CHARACTERISTICS/FINITE ELEMENT METHOD FOR THE INCOMPRESSIBLE NAVIER-STOKES EQUATIONS

K. BOUKIR[1], Y. MADAY[2*], B. MÉTIVET[1] AND E. RAZAFINDRAKOTO[1]

[1] *Electricité de France, DER, 1 Avenue du Général de Gaulle, F-92141 Clamart, France*
[2] *Analyse Numérique—CNRS and Université Pierre et Marie Curie, F-75252 Paris Cedex, 05, France*

SUMMARY

In this paper we consider a discretization of the incompressible Navier–Stokes equations involving a second-order time scheme based on the characteristics method and a spatial discretization of finite element type. Theoretical and numerical analyses are detailed and we obtain stability results and optimal error estimates on the velocity and pressure under a time step restriction less stringent than the standard Courant–Friedrichs–Levy condition. Finally, some numerical results obtained with the code N3S are shown which justify the interest of this scheme and its advantages with respect to an analogous first-order time scheme. © 1997 John Wiley & Sons, Ltd.

Int. J. Numer. Meth. Fluids, **25**: 1421–1454 (1997)

No. of Figures: 8. No. of Tables: 0. No. of References: 29.

KEY WORDS: incompressible Navier–Stokes problem; finite element method; high-order time scheme; method of characteristics

1. INTRODUCTION

In this paper we analyse a high-order-in-time splitting scheme applied to the discretization of the time-dependent Navier–Stokes equations. We consider the following initial value problem: find $\mathbf{u}$: $\Omega\times]0,\ T[\to\mathbb{R}^d$ and p: $\Omega\times]0,\ T[\to\mathbb{R}$ such that

$$\frac{\partial\mathbf{u}}{\partial t}-\nu\Delta\mathbf{u}+\mathbf{u}\cdot\nabla\mathbf{u}+\operatorname{grad}p=\mathbf{f}\quad\text{in }\Omega\times]0,\ T[, \tag{1}$$

$$\operatorname{div}\mathbf{u}=0\quad\text{in }\Omega\times]0,\ T[, \tag{2}$$

$$\mathbf{u}(t=0)=\mathbf{u}_0$$

in some given domain Ω of $\mathbb{R}^d$ ($d=2$ or 3), where the function $\mathbf{f}$ denotes the body forces and $\mathbf{u}_0$ is some given initial condition. We complement these equations with some boundary conditions, e.g.

$$\mathbf{u}=\mathbf{0}\quad\text{on }\partial\Omega. \tag{3}$$

The discretization of these equations is well known to be critical, especially if, which is more and more often the case, high-order discretization is required. We shall focus our attention on the case

CCC 0271–2091/97/121421–34 $17.50

Received 9 December 1992
Revised 24 March 1995

where a finite element spatial discretization together with a second-order time discretization is used. An analogous study with a spectral space discretization is given by Boukir *et al.*[1] The splitting scheme can be obtained using the framework presented in References 2 and 3 to obtain high-order time schemes. Those authors introduce a splitting technique in the general case of a partial differential equation where two or more operators are represented. Some applications of their technique lead to time discretizations of the Stokes and Navier–Stokes equations. Here the splitting scheme consists of a convection step, which is treated using the characteristics method, and a Stokes step. This kind of time discretization is well known under the name of the characteristics method or the Lagrange–Galerkin method.

The current second-order-in-time schemes for the Navier–Stokes equations are generally based on a semi-implicit or explicit treatment of the convection operator (by Crank–Nicolson, Adams–Bashforth, etc. schemes). However, these procedures yield either unsymmetric systems or conditional stability under strong conditions (of the kind $\Delta t \leqslant Ch$). The advantage of the scheme considered in this paper is that it treats the convection operator explicitly and hence yields symmetric systems and provides good stability properties (conditions of the kind $\Delta t \leqslant Ch^{d/2}$ in dimension d).

Actually, the scheme which is studied here is an extension to second order in time of the classical first-order characteristics scheme.[4–9] Note that the latter scheme has been used for years by Benque *et al.*[4,10] Theoretical studies have been investigated in References 5–8. Pironneau[5] has analysed the first-order characteristics scheme together with a finite element method for the Navier–Stokes equations. He obtains unconditional stability results in the case where the characteristics are transported by a divergence-free field that is deduced from the velocity field. The opposite case, where the characteristics are transported by the discrete velocity field, which is not divergence-free, has been treated by Suli,[7] who proves optimal error estimates under some stability condition. Concerning other spatial discretizations together with the first-order scheme, the finite difference method has been treated by Douglas and Russell[6] for the linear convection–diffusion problem and an analysis of the periodic spectral method has been done by Suli and Ware[8,9] for hyperbolic and convection-dominated diffusion problems.

Concerning the second-order scheme, the linear convection–diffusion problem has been analysed by Ewing and Russell[11] and numerical studies have been developed by Boukir *et al.*[12] and Buscaglia and Dari[13] for the Navier–Stokes equations. In the latter case the second-order scheme deals with the computation of two convected velocity fields in the convection step. These are used to discretize the total derivative of the velocity with the help of a backward second-order differentiation scheme, which leads to a Stokes step. The latter is solved by a Uzawa algorithm. We give here theoretical and numerical results for a finite element spatial discretization in the case where the characteristics are transported by a second-order approximation of the discrete velocity field, which is not divergence-free (indeed, owing to the spatial discretization, only the discrete divergence is equal to zero). This is the method that has been implemented in the N3S code developed at Electricité de France.[10] We prove optimal error estimates for velocity (in $l^{\infty}(H^1)$) and pressure in $(l^2(L^2))$. Moreover, we prove H^1 stability under the not too stringent condition $\Delta t \leqslant Ch^{d/6}$, where Δt and h are the time and space steps respectively. Let us note that—as is often the situation, even in the linear case—the error bound and the constant C^{-1} of the stability condition tend exponentially to infinity as the viscosity coefficient ν tends to zero. A more accurate analysis of the influence of the viscosity parameter is presented in Reference 1, where stability results independent of the viscosity coefficient are given. Note also that in this paper the analysis does not take into account the destabilizing effects of numerical quadrature in computing the integrals involving the convected fields.[14–16] To end with, we also present numerical examples treated with the help of N3S which confirm the theoretical results and show the improvements given by the second-order scheme compared with the first-order one for the computation of either steady or transient states. However, this comparison does not deal with the mass preservation property of the two schemes. This point is under investigation.

The outline of the paper is as follows. In Section 2 two equivalent formulations of the time scheme, without spatial discretization, are presented. The consistency error is given. Different methods of discretizing the equations of the characteristics are discussed. We introduce the finite element spatial discretization of the scheme in Section 3. Stability and convergence results of the fully discretized scheme are given in Section 4. Some numerical examples are treated in Section 5.

Notation

The norm of any Banach space E is denoted $\|\cdot\|_E$.

Throughout the paper we work with a domain Ω of $\mathbb{R}^d$ ($d = 2$ or 3) which is assumed to have a sufficiently smooth boundary $\partial\Omega$. On the domain Ω we shall use the $L^2(\Omega)$ scalar product

$$(\phi, \psi) = \int_\Omega \phi(\mathbf{x})\psi(\mathbf{x})\mathrm{d}\mathbf{x}.$$

For any integers (m, p), $p = \infty$ also, we use the Sobolev spaces $W^{m,p}(\Omega)$ (which are denoted $H^m(\Omega)$ in the case $p = 2$, where $L^p(\Omega)$ is the standard Lebesgue space), which are provided with the norms

$$\|\phi\|_{W^{m,p}(\Omega)} = \left(\sum_{\alpha\in\mathbb{R}^d, 0 \leqslant |\alpha| \leqslant m} \|\partial^\alpha \phi\|^p_{L^p(\Omega)} \right)^{1/p} \quad \text{if } 1 \leqslant p < \infty,$$

$$\|\phi\|_{W^{m,\infty}(\Omega)} = \max_{\alpha\in\mathbb{R}^d, 0 \leqslant |\alpha| \leqslant m} \|\partial^\alpha \phi\|_{L^\infty(\Omega)}.$$

We also recall that the seminorm

$$|\phi|_{H^1(\Omega)} = \|\nabla\phi\|_{L^2(\Omega)}$$

is a norm on the space $H^1_0(\Omega)$ of the functions of $H^1(\Omega)$ vanishing on the boundary $\partial\Omega$, which is equivalent to the classical norm of $H^1(\Omega)$. For any fixed positive real $T > 0$ we introduce the time interval $[0, T]$. We denote by $L^\infty(0, T; W^{m,p}(\Omega))$ (resp. $L^2(0, T; W^{m,p}(\Omega))$ the space of the functions $\phi(\mathbf{x}, t)$ defined in $\Omega \times [0, T]$ that belong to $W^{m,p}(\Omega)$ for any t in $[0, T]$ and satisfy

$$\operatorname*{ess\,sup}_{t\in[0,T]} \|\phi(., t)\|_{W^{m,p}(\Omega)} < \infty \quad \left(\text{resp. } \int_0^T \|\phi(.., t)\|^2_{W^{m,p}(\Omega)} < \infty\right).$$

This space is provided with the norm

$$\|\phi\|_{L^\infty(0,T;W^{m,p}(\Omega))} = \operatorname*{ess\,sup}_{t\in[0,T]} \|\phi(., t)\|_{W^{m,p}(\Omega)}$$

$$\left(\text{resp. } \|\phi\|_{L^2(0,T;W^{m,p}(\Omega))} = \left(\int_0^T \|\phi(., t)\|^2_{W^{m,p}(\Omega)}\right)^{1/2}\right).$$

The space of functions in $L^2(\Omega)$ with a zero average is denoted by $L^2_0(\Omega)$.

In mathematical mode, vectorial quantities are indicated by bold type.

2. DISCRETIZATION IN TIME; SECOND-ORDER APPROXIMATION

The basic idea of the splitting technique for approximating the Navier–Stokes equations (1)–(3) is to decouple in the temporal discretization process the convection part from the Stokes part. At each time

step the new velocity and pressure are updated by solving first an equation of convection type of the form

$$\frac{\partial \mathbf{v}}{\partial t} + \mathbf{v} \cdot \nabla \mathbf{v} = 0, \tag{4}$$

then a Stokes equation

$$\frac{\partial \mathbf{v}}{\partial t} - \nu \Delta \mathbf{v} + \operatorname{grad} p = \mathbf{f}, \tag{5}$$

$$\operatorname{div} \mathbf{v} = 0. \tag{6}$$

2.1. Presentation of second-order time scheme

Let us choose a time step $\Delta t > 0$ and define $t^n = n\,\Delta t$ for any $0 \leqslant n \leqslant T/\Delta t = N$. For any function $\mathbf{v}$: $\Omega \times [0, T] \to \mathbb{R}$ we note that

$$\mathbf{v}^n(\mathbf{x}) = \mathbf{v}(\mathbf{x}, t^n). \tag{7}$$

Let $\mathbf{U}^0, \mathbf{U}^n, \ldots, \mathbf{U}^n$ be given in $H_0^1(\Omega$ and assumed to be approximations of $\mathbf{u}^0, \mathbf{u}^1, \ldots, \mathbf{u}^n$, where $\mathbf{u}$ is the solution of the Navier–Stokes problem (1)–(3). The first step consists of defining an approximation $\tilde{\mathbf{U}}^n$ of the solution at time t^{n+1} of equation (4) provided with the initial condition at time t^n

$$\mathbf{v}(t = t^n) = \mathbf{U}^n. \tag{8}$$

This is done by defining a convective velocity $\mathbf{U}^{n*}$ (e.g. we can choose $\mathbf{U}^{n*} = 2\mathbf{U}^n - \mathbf{U}^{n-1}$ or $\mathbf{U}^{n*}(t) = (1/\Delta t)[(t^n - t)\mathbf{U}^{n-1} + (t - t^{n-1})\mathbf{U}^n]$). Then we set

$$\tilde{\mathbf{U}}^n(\mathbf{x}) = \boldsymbol{\varphi}(\mathbf{x}, t^{n+1}), \tag{9}$$

where $\boldsymbol{\varphi}$: $\Omega \times [t^n, t^{n+1}] \to \mathbb{R}^d$ is the solution of the passive convection problem

$$\begin{aligned} \frac{\partial \boldsymbol{\varphi}}{\partial t} &= -\mathbf{U}^{n*} \cdot \nabla \boldsymbol{\varphi} \quad \text{in } \Omega \times]t^n, t^{n+1}], \\ \boldsymbol{\varphi}(\mathbf{x}, t^n) &= \mathbf{U}^n(\mathbf{x}), \quad \mathbf{x} \in \Omega, \\ \boldsymbol{\varphi} &= 0 \quad \text{on } \partial\Omega. \end{aligned} \tag{10}$$

Similarly, an approximation $\tilde{\tilde{\mathbf{U}}}^{n-1}$ at time t^{n+1} of the solution of (4) with the initial condition at time t^{n-1},

$$\mathbf{v}(t = t^{n-1}) = \mathbf{U}^{n-1}, \tag{11}$$

is given by

$$\tilde{\tilde{\mathbf{U}}}^{n-1}(\mathbf{x}) = \boldsymbol{\psi}(\mathbf{x}, t^{n+1}), \tag{12}$$

where $\boldsymbol{\psi}$: $\Omega \times [t^{n-1}, t^{n+1}] \to \mathbb{R}^d$ is the solution of the problem

$$\begin{aligned} \frac{\partial \boldsymbol{\psi}}{\partial t} &= -\mathbf{U}^{n*} \cdot \nabla \boldsymbol{\psi} \quad \text{in } \Omega \times]t^{n-1}, t^{n+1}], \\ \boldsymbol{\psi}(\mathbf{x}, t^{n-1}) &= \mathbf{U}^{n-1}(\mathbf{x}), \quad \mathbf{x} \in \Omega, \\ \boldsymbol{\psi} &= 0 \quad \text{on } \partial\Omega. \end{aligned} \tag{13}$$

These two approximations are then used in order to define an approximation $(\mathbf{U}^{n+1}, P^{n+1})$ of $(\mathbf{u}^{n+1}, p^{n+1})$ by solving a Stokes problem: find $\mathbf{U}^{n+1}: \Omega \to \mathbb{R}^d$ and $P^{n+1}: \Omega \to \mathbb{R}$ such that

$$\frac{3\mathbf{U}^{n+1} - 4\tilde{\mathbf{U}}^{n} + \tilde{\tilde{\mathbf{U}}}^{n-1}}{2\Delta t} - \nu\Delta\mathbf{U}^{n+1} + \nabla P^{n+1} = \mathbf{f}^{n+1} \quad \text{in } \Omega, \tag{14}$$

$$\operatorname{div} \mathbf{U}^{n+1} = 0 \quad \text{in } \Omega, \tag{15}$$

$$\mathbf{U}^{n+1} = 0 \quad \text{over } \partial\Omega. \tag{16}$$

It is an easy matter to check that (9)–(16) provide a recurrent approximation $(\mathbf{U}^{n+1}, P^{n+1})$ of the solution $(\mathbf{u}, p)$.

As already explained by Maday *et al.*,[3] this splitting scheme is a second-order characteristics method in the same spirit as the scheme analysed by Ewing and Russell.[11] To understand this, we introduce for any given $\mathbf{x}$ in Ω the characteristic curve $\mathbf{X}_{\mathbf{x}}^{n+1}$ defined by

$$\mathbf{X}_{\mathbf{x}}^{n+1}: [t^{n-1}, t^{n+1}] \to \bar{\Omega},$$

the solution of (the backward problem)

$$\frac{d\mathbf{X}_{\mathbf{x}}^{n+1}}{dt} = \mathbf{U}^{n*}(\mathbf{X}_{\mathbf{x}}^{n+1}(t)) \quad \text{in } [t^{n-1}, t^{n+1}[,$$
$$\mathbf{X}_{\mathbf{x}}^{n+1}(t^{n+1}) = \mathbf{x}. \tag{17}$$

Since $\mathbf{U}^{n*} = 0$ on $\partial\Omega$, we have $\mathbf{X}_{\mathbf{x}}^{n+1}(t) \in \Omega$. We then verify easily the following lemma.

Lemma 1

The quantities $\tilde{\mathbf{U}}^{n}(\mathbf{x})$ and $\tilde{\tilde{\mathbf{U}}}^{n-1}(\mathbf{x})$ are the values of $\mathbf{U}^{n}$ and $\mathbf{U}^{n-1}$ respectively at two feet of the characteristic curve $\mathbf{X}_{\mathbf{x}}^{n+1}$ in the following sense:

$$\tilde{\mathbf{U}}^{n}(\mathbf{x}) = \mathbf{U}^{n}(\mathbf{X}_{\mathbf{x}}^{n+1}(t^{n})), \tag{18}$$

$$\tilde{\tilde{\mathbf{U}}}^{n-1}(\mathbf{x}) = \mathbf{U}^{n-1}(\mathbf{X}_{\mathbf{x}}^{n+1}(t^{n-1})). \tag{19}$$

From now on we shall use the notation $\mathbf{U}^{n*} = 2\mathbf{U}^{n} - \mathbf{U}^{n-1}$. We define $\mathbf{u}^{n*}$ and $\chi_{\mathbf{x}}^{n+1}$ in a similar way as $\mathbf{U}^{n*}$ and $\mathbf{X}_{\mathbf{x}}^{n+1}$ but with the help of the continuous solution of (1)–(3). Then we set

$$\tilde{\mathbf{u}}^{n}(\mathbf{x}) = \mathbf{u}^{n}(\chi_{\mathbf{x}}^{n+1}(t^{n})), \tag{20}$$

$$\tilde{\tilde{\mathbf{u}}}^{n-1}(\mathbf{x}) = \mathbf{u}^{n-1}(\chi_{\mathbf{x}}^{n+1}(t^{n-1})). \tag{21}$$

2.2. *Consistency properties*

Our concern now is to prove that (9)–(16) provide a second-order approximation of the solution $(\mathbf{u}, p)$ of the Navier–Stokes equations (1)–(3). For this purpose let us first analyse the consistency error

$$\mathbf{e}(\mathbf{x}, n+1) = \left(\frac{3\mathbf{u}^{n+1} - 4\tilde{\mathbf{u}}^{n} + \tilde{\tilde{\mathbf{u}}}^{n-1}}{2\Delta t} - \nu\Delta\mathbf{u}^{n+1} + \nabla p^{n+1} - \mathbf{f}^{n+1}\right)(\mathbf{x}),$$

which from (1) is equal to

$$\mathbf{e}(\mathbf{x}, n+1) = \left[\frac{3\mathbf{u}^{n+1} - 4\tilde{\mathbf{u}}^{n} + \tilde{\tilde{\mathbf{u}}}^{n-1}}{2\Delta t} - \left(\frac{\partial \mathbf{u}}{\partial t}(t^{n+1}) + \mathbf{u}^{n+1} \cdot \nabla \mathbf{u}^{n+1}\right)\right](\mathbf{x}). \tag{22}$$

Lemma 2

Let $\tau > 0$ be such that $\mathbf{u} \in [\mathscr{C}^4([\tau,\ T] \times \bar{\Omega})]^d$. For $t^{n+1} > \tau$ we have

$$\mathbf{e}(\mathbf{x}, n+1) = -\Delta t^2 \left(\frac{1}{3}\frac{\mathrm{d}^3 \mathbf{h}_{\mathbf{x}}^{n+1}}{\mathrm{d}t^3}(t^{n+1}) + \frac{\partial^2 \mathbf{u}}{\partial t^2} \cdot \nabla \mathbf{u}(\mathbf{x}, t^{n+1})\right) + O(\Delta t^3), \tag{23}$$

where

$$\mathbf{h}_{\mathbf{x}}^{n+1}(t) = \mathbf{u}(\chi_{\mathbf{x}}^{n+1}(t), t). \tag{24}$$

Proof. We immediately check that

$$\frac{\mathrm{d}\mathbf{h}_{\mathbf{x}}^{n+1}}{\mathrm{d}t}(t^{n+1}) = \frac{\partial \mathbf{u}}{\partial t}(\mathbf{x}, t^{n+1}) + \mathbf{u}^{n*}(\mathbf{x}) \cdot \nabla \mathbf{u}^{n+1}(\mathbf{x}). \tag{25}$$

It follows from (20)–(22), (24) and (25) that

$$\mathbf{e}(\mathbf{x}, n+1) = \left(\frac{3\mathbf{h}_{\mathbf{x}}^{n+1}(t^{n+1}) - 4\mathbf{h}_{\mathbf{x}}^{n+1}(t^{n}) + \mathbf{h}_{\mathbf{x}}^{n+1}(t^{n-1})}{2\Delta t} - \frac{\mathrm{d}\mathbf{h}_{\mathbf{x}}^{n+1}}{\mathrm{d}t}(t^{n+1})\right) + [(\mathbf{u}^{n*} - \mathbf{u}^{n+1}) \cdot \nabla \mathbf{u}^{n+1}](\mathbf{x}). \tag{26}$$

The first term of (26) represents the consistency error of the standard second-order backward differentiation; thus

$$\frac{3\mathbf{h}_{\mathbf{x}}^{n+1}(t^{n+1}) - 4\mathbf{h}_{\mathbf{x}}^{n+1}(t^{n}) + \mathbf{h}_{\mathbf{x}}^{n+1}(t^{n-1})}{2\Delta t} - \frac{\mathrm{d}\mathbf{h}_{\mathbf{x}}^{n+1}}{\mathrm{d}t}(t^{n+1}) = -\frac{1}{3}\Delta t^2 \frac{\mathrm{d}^3 \mathbf{h}_{\mathbf{x}}^{n+1}}{\mathrm{d}t^3}(t^{n+1}) + O(\Delta t^3). \tag{27}$$

Moreover, $\mathbf{u}^{n*} = 2\mathbf{u}^{n} - \mathbf{u}^{n-1}$ is a standard second-order approximation of $\mathbf{u}^{n+1}$: we have

$$\mathbf{u}^{n*} - \mathbf{u}^{n+1} = -\Delta t^2 \left(\frac{\partial^2 \mathbf{u}}{\partial t^2}\right)(., t^{n+1}) + O(\Delta t^3). \tag{28}$$

Combining (27) and (28) leads to (23).

Remark 1

Actually, the notation $O(\Delta t^3)$ is a quantity depending on $\mathbf{x}$ but which is uniformly bounded on Ω with respect to $\mathbf{x}$.

Remark 2

Lemma 2 tells us that $(3\mathbf{U}^{n+1} - 4\tilde{\mathbf{U}}^{n} + \tilde{\tilde{\mathbf{U}}}^{n-1})/2\Delta t$ is a second-order backward differentiation approximation of the total derivative $\mathrm{d}\mathbf{u}/\mathrm{d}t = \partial \mathbf{u}/\partial t + \mathbf{u} \cdot \nabla \mathbf{u}$. The expression (26) can also explain why $\mathbf{U}^{n*} = 2\mathbf{U}^{n} - \mathbf{U}^{n-1}$ is the only linear constant coefficient combination of $\mathbf{U}^{n}$ and $\mathbf{U}^{n-1}$ that gives a

second-order scheme. Of course we could have used $(1/\Delta t)[(t^n - t)\mathbf{U}^{n-1} + (t - t^{n-1})\mathbf{U}^n]$ instead of $\mathbf{U}^{n*}(t)$; this would have led to a second-order approximation as well.[3]

Remark 3

Note that the above scheme is defined using only one characteristic curve that is defined using only one characteristic curve that is defined on an interval of size $2\Delta t$. Then two feet of this characteristic curve are used to define the convected fields (18) and (19). We give here another procedure to define these fields which also leads to a second-order global scheme.[14] At each time step we compute a characteristic curve that is defined on an interval only of size Δt as

$$\mathbf{X}_{\mathbf{x}}^{n+1}: [t^n, t^{n+1}] \to \bar{\Omega},$$

the solution of (the backward problem)

$$\frac{\mathrm{d}\mathbf{X}_{\mathbf{x}}^{n+1}}{\mathrm{d}t} = \mathbf{U}^{n+}(\mathbf{X}_{\mathbf{x}}^{n+1}(t)) \quad \text{in } [t^n, t^{n+1}[,$$
$$\mathbf{X}_{\mathbf{x}}^{n+1}(t^{n+1}) = \mathbf{x},$$

where in this case

$$\mathbf{U}^{n+} = \tfrac{3}{2}\mathbf{U}^n - \tfrac{1}{2}\mathbf{U}^{n-1}.$$

The convected velocity fields are then given by

$$\tilde{U}^n(x) = U^n(X_x^{n+1}(t^n)),$$
$$\tilde{\tilde{U}}^{n-1}(x) = U^{n-1}(X^n_{X_x^{n+1}(t^n)}(t^{n-1})) = \tilde{U}^{n-1}(X_x^{n+1}(t^n)),$$

where the characteristic curve $\mathbf{X}_{\mathbf{y}}^n$, $\mathbf{y} \in \Omega$ (here $\mathbf{y} = \mathbf{X}_{\mathbf{x}}^{n+1}(t^n)$), is defined using the velocity $\mathbf{U}^{(n-1)+}$ and assumed to be already computed in the previous time step t^n. This method seems efficient for approximating the total derivative $\mathrm{d}\mathbf{u}/\mathrm{d}t = \partial\mathbf{u}/\partial t + \mathbf{u}\cdot\nabla\mathbf{u}$; in this way the continuous characteristic curve could be approximated more accurately. Note also its good properties of induction which allow us to obtain stability results independent of the viscosity coefficient[1] for the linear convection–diffusion problem.

2.3. Discretization of characteristics

From now on, with any sequence $(\mathbf{v}^n)_n$ we associate $\mathbf{v}^{n*}$ defined by

$$\mathbf{v}^{n*} = 2\mathbf{v}^n - \mathbf{v}^{n-1}.$$

In practice, in (18) and (19) the feet of the characteristics $\mathbf{X}_{\mathbf{x}}^{n+1}(t^n)$ and $\mathbf{X}_{\mathbf{x}}^{n+1}(t^{n-1})$ are not computed exactly. We denote by $\underline{\mathbf{x}}$ and $\underline{\underline{\mathbf{x}}}$ any approximation of these quantities,

$$\underline{\mathbf{x}} \sim \mathbf{X}_{\mathbf{x}}^{n+1}(t^n), \tag{29}$$
$$\underline{\underline{\mathbf{x}}} \sim \mathbf{X}_{\mathbf{x}}^{n+1}(t^{n-1}), \tag{30}$$

and consequently we obtain approximations $\underline{\mathbf{U}}^n$ and $\underline{\underline{\mathbf{U}}}^{n-1}$ of the convected fields $\tilde{\mathbf{U}}^n$ and $\tilde{\tilde{\mathbf{U}}}^{n-1}$ respectively defined by

$$\underline{\mathbf{U}}^n(\mathbf{x}) = \begin{cases} \mathbf{U}^n(\underline{\mathbf{x}}) & \text{if } \underline{\mathbf{x}} \in \bar{\Omega}, \\ 0 & \text{otherwise;} \end{cases} \tag{31}$$

$$\underline{\underline{\mathbf{U}}}^{n-1} = \begin{cases} \mathbf{U}^{n-1}(\underline{\underline{\mathbf{x}}}) & \text{if } \underline{\underline{\mathbf{x}}} \in \bar{\Omega}, \\ 0 & \text{otherwise.} \end{cases} \tag{32}$$

Actually, the notations $\underline{\mathbf{x}}$ and $\underline{\underline{\mathbf{x}}}$ are improper, as they should be denoted $\underline{\mathbf{x}}^{n+1}$ and $\underline{\underline{\mathbf{x}}}^{n+1}$ respectively. For the sake of convenience, however, we shall suppress the superscript, making it implicit in the use.

Replacing $\tilde{\mathbf{U}}^n$ and $\tilde{\tilde{\mathbf{U}}}^{n-1}$ in (14) by $\underline{\mathbf{U}}^n$ and $\underline{\underline{\mathbf{U}}}^{n-1}$ respectively, we obtain a new scheme. We are interested here in approximations that preserve the second-order accuracy of the global scheme (9)–(16).

We focus our study on a first-order approximation suggested by Ewing and Russell;[11] we set

$$\underline{\mathbf{x}} = \mathbf{x} - \mathbf{U}^{n*}(\mathbf{x})\Delta t, \tag{33}$$

$$\underline{\underline{\mathbf{x}}} = \mathbf{x} - 2\mathbf{U}^{n*}(\mathbf{x})\Delta t. \tag{34}$$

We define $\underline{\mathbf{u}}^n$ and $\underline{\underline{\mathbf{u}}}^{n-1}$ in similar way as $\underline{\mathbf{U}}^n$ and $\underline{\underline{\mathbf{U}}}^{n-1}$ using the approximation (33), (34):

$$\underline{\mathbf{u}}^n(\mathbf{x}) = \begin{cases} \mathbf{u}^n(\underline{\mathbf{x}}) & \text{if } \underline{\mathbf{x}} = \mathbf{x} - \mathbf{u}^{n*}(\mathbf{x})\Delta t \in \bar{\Omega}, \\ 0 & \text{otherwise,} \end{cases} \tag{35}$$

$$\underline{\underline{\mathbf{u}}}^{n-1} = \begin{cases} \mathbf{u}^{n-1}(\underline{\underline{\mathbf{x}}}) & \text{if } \underline{\underline{\mathbf{x}}} = \mathbf{x} - 2\mathbf{u}^{n*}(\mathbf{x})\Delta t \in \bar{\Omega}, \\ 0 & \text{otherwise.} \end{cases} \tag{36}$$

We can check that the consistency error

$$\underline{\mathbf{e}}(\mathbf{x}, n+1) = \left(\frac{3\mathbf{u}^{n+1} - 4\underline{\mathbf{u}}^n + \underline{\underline{\mathbf{u}}}^{n-1}}{2\Delta t} - \nu\Delta\mathbf{u}^{n+1} + \nabla p^{n+1} - \mathbf{f}^{n+1}\right)(\mathbf{x})$$

is also of second-order accuracy.

Lemma 3

Let $\tau > 0$ be such that $\mathbf{u} \in [\mathscr{C}^4([\tau, T] \times \bar{\Omega})]^d$. We have

$$\underline{\mathbf{e}}(\mathbf{x}, n+1) = -\Delta t^2\left(\frac{1}{3}\frac{\mathrm{d}^3\mathbf{g}_{\mathbf{x}}^{n+1}}{\mathrm{d}t^3}(t^{n+1}) + \frac{\partial^2\mathbf{u}}{\partial t^2}\cdot\nabla\mathbf{u}(\mathbf{x}, t^{n+1})\right) + O(\Delta t^3),$$

where

$$\mathbf{g}_{\mathbf{x}}^{n+1}(t) = \mathbf{u}(\mathbf{x} - (t^{n+1} - t)\mathbf{u}^{n*}(\mathbf{x}), t). \tag{37}$$

The proof of this result is similar to the proof of Lemma 2 with $\mathbf{h}$ replaced by $\mathbf{g}$.

The particularity of the procedure (33), (34) is that (17) is approximated by a first-order scheme that does not pollute the second-order accuracy of the global scheme (9)–(16).

In what follows we shall use a bound of the consistency error in the $L^2(\Omega)$-norm. This is obtained by following the same lines as in the previous proofs under a less stringent regularity assumption on $\mathbf{u}$ using a Taylor formula with an integral remainder. This is stated in the following lemma.

Lemma 4

Let $\tau > 0$ be such that

$$\mathbf{u} \in L^\infty(\tau, T; W^{1,\infty}(\Omega)), \qquad \frac{\partial^2\mathbf{u}}{\partial t^2} \in L^2(\tau, T; L^2(\Omega)), \qquad \frac{\mathrm{d}^3\mathbf{g}_{\mathbf{x}}^{n+1}}{\mathrm{d}t^3} \in L^2(\tau, T; L^2(\Omega))$$

hold, where $\mathbf{g}_{\mathbf{x}}^{n+1}$ is defined as in (37). We have

$$\sum_{n=2}^{N} \Delta t \|\underline{\mathbf{e}}(.,n)\|^2_{L^2(\Omega)} \leqslant C(\mathbf{u},T)\Delta t^4 \tag{38}$$

Remark 4

(i) Another first-order approximation of (17) could be considered by setting

$$\underline{\underline{\mathbf{x}}} = \underline{\mathbf{x}} - \mathbf{U}^{n*}(\underline{\mathbf{x}})\Delta t, \tag{39}$$

where $\underline{\mathbf{x}}$ is defined as in (33). This modified procedure allows us to bend the discrete characteristic curve and thus follow more accurately the continuous one than does the approximation (33), (34). However, it is shown that the second-order accuracy of the global scheme is lost in this way and yields to a first-order approximation.[11]

(ii) The approximation (33), (34) combined with a multistep method bends more efficiently the discrete characteristic curve and leads to more accurate discrete feet $\underline{\mathbf{x}}$ and $\underline{\underline{\mathbf{x}}}$. For any positive integers $l>0$ and $l'>0$ we define the substeps $\delta t=\Delta t/l$ and $\delta t'=\Delta t/l'$ and we set for $1 \leqslant i \leqslant l$ and $1 \leqslant j \leqslant l'$

$$\begin{aligned} &\underline{\mathbf{x}}_0 = \mathbf{x}, && \underline{\underline{\mathbf{x}}}_0 = \mathbf{x}, \\ &\underline{\mathbf{x}}_i = \underline{\mathbf{x}}_{i-1} - \mathbf{U}^{n*}(\underline{\mathbf{x}}_{i-1})\delta t, && \underline{\underline{\mathbf{x}}}_j = \underline{\underline{\mathbf{x}}}_{j-1} - \mathbf{U}^{n*}(\underline{\underline{\mathbf{x}}}_{j-1})\delta t', \\ &\underline{\mathbf{x}} = \underline{\mathbf{x}}_l, && \underline{\underline{\mathbf{x}}} = \underline{\underline{\mathbf{x}}}_{l'}. \end{aligned} \tag{40}$$

We can show[14] that if we use the same number of substeps ($l=l'$) for the computation of the two feet $\underline{\mathbf{x}}$ and $\underline{\underline{\mathbf{x}}}$, we obtain a second-order global scheme. However, we remark that for $l=1$ and $l'=2$ we get the above modified procedure (39).

(iii) Note that any second-order approximation of (17) preserves the second-order accuracy of the global scheme.[14] For instance, the use of a second-order Runge–Kutta scheme allows us to compute $\underline{\mathbf{x}}$ and $\underline{\underline{\mathbf{x}}}$ as well as bend the characteristic curve in the same spirit as in (39). We set

$$\underline{\mathbf{x}} = \mathbf{x} - \mathbf{U}^{n*}(\underline{\mathbf{x}}^1)\Delta t, \quad \text{where} \quad \underline{\mathbf{x}}^1 = \mathbf{x} - \mathbf{U}^{n*}(\mathbf{x})\frac{\Delta t}{2}, \tag{41}$$

$$\underline{\underline{\mathbf{x}}} = \underline{\mathbf{x}} - \mathbf{U}^{n*}(\underline{\underline{\mathbf{x}}}^1)\Delta t, \quad \text{where} \quad \underline{\underline{\mathbf{x}}}^1 = \underline{\mathbf{x}} - \mathbf{U}^{n*}(\underline{\mathbf{x}})\frac{\Delta t}{2}. \tag{42}$$

If more accurate approximations of these feet are required, we can also apply a multistep method to (41), (42) in the same spirit as in (40). We define $1 \leqslant i \leqslant l$ and $1 \leqslant j \leqslant l'$

$$\begin{aligned} &\underline{\mathbf{x}}_0 = \mathbf{x}, \\ &\underline{\mathbf{x}}_i = \underline{\mathbf{x}}_{i-1} - \mathbf{U}^{n*}(\underline{\mathbf{x}}^1_{i-1})\delta t, \quad \text{where} \quad \underline{\mathbf{x}}^1_{i-1} = \underline{\mathbf{x}}_{i-1} - \mathbf{U}^{n*}(\underline{\mathbf{x}}^1_{i-1})\frac{\delta t}{2}, \\ &\underline{\mathbf{x}} = \underline{\mathbf{x}}_l, \end{aligned} \tag{43}$$

$$\begin{aligned} &\underline{\underline{\mathbf{x}}}_0 = \underline{\mathbf{x}}, \\ &\underline{\underline{\mathbf{x}}}_j = \underline{\underline{\mathbf{x}}}_{j-1} - \mathbf{U}^{n*}(\underline{\underline{\mathbf{x}}}^1_{j-1})\delta t', \text{ where } \underline{\underline{\mathbf{x}}}^1_{j-1} = \underline{\underline{\mathbf{x}}}_{j-1} - \mathbf{U}^{n*}(\underline{\underline{\mathbf{x}}}_{j-1})\frac{\delta t'}{2}, \\ &\underline{\underline{\mathbf{x}}} = \underline{\underline{\mathbf{x}}}_{l'}. \end{aligned} \tag{44}$$

Here l and l' are chosen independently.

In the next sections we prove that the semidiscretization (9)–(16) combined with a spatial discretization is stable under some condition between the time step and the spatial discrete parameter. We do not know currently how to prove that the semidiscrete scheme (9)–(16) is stable.

3. PRESENTATION OF FULLY DISCRETE PROBLEM

The semidiscretization (9)–(16) is completed by a spatial discretization that can be either of finite difference, spectral element[1] of finite element type. Here we shall investigate the properties of the latter as regards stability and convergence. The basics of the finite element discretization are first a triangulation into K non-overlapping elements T^l, $1 \leqslant l \leqslant K$. We denote by h_l the diameter of T^l and we introduce the space step $h = \sup_{1 \leqslant l \leqslant K} h_l$. We suppose the triangulation to be uniformly regular.

If the elements are triangles or tetrahedra, $\mathscr{P}^k$ represents the set of all polynomials of global degree $\leqslant k$; if the elements are rectangles or hexahedra, $\mathscr{P}^k$ represents the set of all polynomials of degree $\leqslant k$ with respect to each space variable. We can now define the approximation spaces

$$Y_h = \{\varphi \in C^0(\bar{\Omega});\ \varphi|_{T^l} \in \mathscr{P}^k(T^l),\ 1 \leqslant l \leqslant K\}, \tag{45}$$

$$Q_h = \{\varphi \in L_0^2(\Omega);\ \varphi|_{T^l} \in \mathscr{P}^{k'}(T^l),\ 1 \leqslant l \leqslant K\}. \tag{46}$$

The space $[H_0^1(\Omega)]^d$ is then approximated by

$$X_h = [Y_h \cap H_0^1(\Omega)]^d. \tag{47}$$

We assume that the degrees k and k' are chosen such that (X_h, Q_h) satisfies the inf-sup condition

$$\inf_{q_h \in Q_h - \{0\}} \sup_{\mathbf{v}_h \in X_h} \frac{(\nabla \cdot \mathbf{v}_h, q_h)}{\|\mathbf{v}_h\|_{H^1(\Omega)} \|q_h\|_{L^2(\Omega)}} \geqslant \beta > 0. \tag{48}$$

More precisely, let V_h denote the kernel of the discrete divergence operator,

$$V_h = \{\mathbf{v}_h \in X_h;\ (\nabla \cdot \mathbf{v}_h, q_h) = 0, \forall q_h \in Q_h\}, \tag{49}$$

and $V = \{\mathbf{v} \in [H_0^1(\Omega)]^d;\ \nabla \cdot \mathbf{v} = 0\}$. It is first obvious that $V \cap X_h \subset V_h$. Besides, let $\Pi_{0,h}^1$ denote the projection operator from V onto V_h defined as

$$(\nabla(\mathbf{v} - \Pi_{0,h}^1 \mathbf{v}), \nabla \mathbf{v}_h) = 0, \quad \forall \mathbf{v}_h \in V_h. \tag{50}$$

Thanks to (48), we have for $1 \leqslant r \leqslant k+1$ the estimate[17]

$$\forall \mathbf{v} \in V \cap [H^r(\Omega)]^d, \quad \|\mathbf{v} - \Pi_{0,h}^1 \mathbf{v}\|_{L^2(\Omega)} + h\|\mathbf{v} - \Pi_{0,h}^1 \mathbf{v}\|_{H^1(\Omega)} \leqslant Ch^r \|\mathbf{v}\|_{H^r(\Omega)}. \tag{51}$$

We have also the $W^{1,\infty}(\Omega)$ and $L^\infty(\Omega)$ bounds for $\mathbf{v} \in [H^{k+1}(\Omega)]^d$ as

$$\|\Pi_{0,h}^1 \mathbf{v}\|_{W^{1,\infty}(\Omega)} \leqslant C(\|\mathbf{v}\|_{W^{1,\infty}(\Omega)} + h^{k-d/2} \|\mathbf{v}\|_{H^{k+1}(\Omega)}), \tag{52}$$

$$\|\Pi_{0,h}^1 \mathbf{v}\|_{L^\infty(\Omega)} \leqslant C(\|\mathbf{v}\|_{L^\infty(\Omega)} + h^{k+1-d/2} \|\mathbf{v}\|_{H^{k+1}(\Omega)}), \tag{53}$$

where C is a constant independent of h but depending on Ω. These results are certainly not optimal but are sufficient for our purpose.

To show the result (52), for instance, we introduce the interpolation operator I_h and the element $I_h\mathbf{v}$. We have from the triangle inequality

$$\|\Pi^1_{0,h}\mathbf{v}\|_{W^{1,\infty}(\Omega)} \leqslant \|I_h\mathbf{v}\|_{W^{1,\infty}(\Omega)} + \|\Pi^1_{0,h}\mathbf{v} - I_h\mathbf{v}\|_{W^{1,\infty}(\Omega)},$$

which, using the inverse inequality[18] $\|\mathbf{v}_h\|_{W^{1,\infty}(\Omega)} \leqslant Ch^{-d/2}\|\mathbf{v}_h\|_{H^1(\Omega)}$, yields

$$\begin{aligned}\|\Pi^1_{0,h}\mathbf{v}\|_{W^{1,\infty}(\Omega)} &\leqslant \|I_h\mathbf{v}\|_{W^{1,\infty}(\Omega)} + Ch^{-d/2}\|\Pi^1_{0,h}\mathbf{v} - I_h\mathbf{v}\|_{H^1(\Omega)} \\ &\leqslant \|I_h\mathbf{v}\|_{W^{1,\infty}(\Omega)} + Ch^{-d/2}(\|\Pi^1_{0,h}\mathbf{v} - \mathbf{v}\|_{H^1(\Omega)} + \|\mathbf{v} - I_h\mathbf{v}\|_{H^1(\Omega)}).\end{aligned}$$

From (51), the H^1 error estimate and the $W^{1,\infty}$ stability property of the interpolation operator[18] we deduce (52).

Let Π'_h denote the projection operator from $L^2(\Omega)$ into Q_h defined as

$$(\Pi'_h q - q, q_h) = 0, \quad \forall q_h \in Q_h. \tag{54}$$

We have for $1 \leqslant s \leqslant k'+1$ the estimate[17]

$$\forall q \in L^2_0(\Omega) \cap H^s(\Omega), \quad \|q - \Pi'_h q\|_{L^2(\Omega)} \leqslant Ch^s\|q\|_{H^s(\Omega)}. \tag{55}$$

The fully discrete scheme can now be defined. Let $(\mathbf{U}^0_h, P^0_h), \ldots, (\mathbf{U}^n_h, P^n_h)$ be given in $V_h \times Q_h$ and as in Section 2 let us associate a convective velocity $\mathbf{U}^{n*}_h = 2\mathbf{U}^n_h - \mathbf{U}^{n-1}_h$. We first define the characteristic curves as solutions of (17) with $\mathbf{U}^{n*}_h$ instead of $\mathbf{U}^{n*}$ and set

$$\overline{\mathbf{U}}^n_h(\mathbf{x}) \simeq \mathbf{U}^n_h(\mathbf{X}^{n+1}_{\mathbf{x}}(t^n)), \tag{56}$$

$$\overline{\overline{\mathbf{U}}}^{n-1}_h(\mathbf{x}) \simeq \mathbf{U}^{n-1}_h(\mathbf{X}^{n+1}_{\mathbf{x}}(t^{n-1})), \tag{57}$$

where the symbol $\simeq$ indicates that some time discretization of the characteristic curve (or convection problem) is added; for instance, following the suggestion of Ewing and Russell,[11] we can set

$$\overline{\mathbf{U}}^n_h(\mathbf{x}) = \mathbf{U}^n_h(\bar{\mathbf{x}}), \quad \text{where } \bar{\mathbf{x}} = \mathbf{x} - \Delta t\mathbf{U}^{n*}_h(\mathbf{x}), \tag{58}$$

$$\overline{\overline{\mathbf{U}}}^{n-1}_h(\mathbf{x}) = \mathbf{U}^{n-1}_h(\bar{\bar{\mathbf{x}}}), \quad \text{where } \bar{\bar{\mathbf{x}}} = \mathbf{x} - 2\Delta t\mathbf{U}^{n*}_h(\mathbf{x}), \tag{59}$$

or any other discretization that preserves the second-order accuracy in time. From now on we shall use (58) and (59).

The solution $(\mathbf{U}^{n+1}_h, P^{n+1}_h) \in X_h \times Q_h$ is then computed by solving the Stokes problem

$$\begin{aligned}&\left(\frac{3\mathbf{U}^{n+1}_h - 4\overline{\mathbf{U}}^n_h + \overline{\overline{\mathbf{U}}}^{n-1}_h}{2\Delta t}, \mathbf{v}_h\right) + \nu(\nabla\mathbf{U}^{n+1}_h, \nabla\mathbf{v}_h) - (\nabla\cdot\mathbf{v}_h, P^{n+1}_h) = (\mathbf{f}^{n+1}, \mathbf{v}_h), \quad \forall\mathbf{v}_h \in X_h, \\ &(\nabla\cdot U^{n+1}_h, q_h) = 0, \quad \forall q_h \in Q_h.\end{aligned} \tag{60}$$

In the next section the notation bar (or double bar) upon any function $\mathbf{v}^n$ denotes as in (58) and (59) the values at the feet of the discrete characteristic curve defined with the velocity $\mathbf{U}^{n*}_h$ (and not with $\mathbf{v}^{n*}$) such that

$$\bar{\mathbf{v}}^n(\mathbf{x}) = \mathbf{v}^n(\bar{\mathbf{x}}), \quad \text{where } \bar{\mathbf{x}} = \mathbf{x} - \Delta t\mathbf{U}^{n*}_h(\mathbf{x}), \tag{61}$$

$$\bar{\bar{\mathbf{v}}}^{n-1}(\mathbf{x}) = \mathbf{v}^{n-1}(\bar{\bar{\mathbf{x}}}), \quad \text{where } \bar{\bar{\mathbf{x}}} = \mathbf{x} - 2\Delta t\mathbf{U}^{n*}_h(\mathbf{x}). \tag{62}$$

4. ANALYSIS OF DISCRETE PROBLEM

4.1. Preliminaries

Let n be a fixed number, $2 \leqslant n \leqslant N$; we introduce or recall the notations

$$\mathbf{w}_h(t) = \Pi^1_{0,h}\mathbf{u}(t), \tag{63}$$

$$\boldsymbol{\eta}(t) = \mathbf{u}(t) - \mathbf{w}_h(t) = \mathbf{u}(t) - \Pi^1_{0,h}\mathbf{u}(t), \tag{64}$$

$$\mathbf{w}_h^n = \mathbf{w}_h(t^n) = \Pi^1_{0,h}\mathbf{u}(t^n), \tag{65a}$$

$$\boldsymbol{\eta}^n = \boldsymbol{\eta}(t^n) = \mathbf{u}(t^n) - \Pi^1_{0,h}\mathbf{u}(t^n), \tag{65b}$$

$$\mathbf{u}^n = \mathbf{u}(t^n), \tag{65c}$$

$$\boldsymbol{\xi}^n = \mathbf{U}_h^n - \mathbf{w}_h^n = \mathbf{U}_h^n - \Pi^1_{0,h}\mathbf{u}(t^n), \tag{66}$$

where $\Pi^1_{0,h}$ is defined as in (50). For the sake of convenience, in the sequel we use the notations

$$\underline{\mathbf{u}}^n(\mathbf{x}) = \mathbf{u}^n(\underline{\mathbf{x}}), \quad \text{where } \underline{\mathbf{x}} = \mathbf{x} - \mathbf{u}^{n*}(\mathbf{x})\Delta t, \tag{67a}$$

$$\underline{\underline{\mathbf{u}}}^{n-1}(\mathbf{x}) = \mathbf{u}^{n-1}(\underline{\underline{\mathbf{x}}}), \quad \text{where } \underline{\underline{\mathbf{x}}} = \mathbf{x} - 2\mathbf{u}^{n*}(\mathbf{x})\Delta t. \tag{67b}$$

Moreover, we recall that the notations $\bar{\mathbf{x}}$, $\bar{\bar{\mathbf{x}}}$ and $\bar{\mathbf{u}}^n$, $\bar{\bar{\mathbf{u}}}^{n-1}$ have been introduced in (61) and (62).

It is well known[9,20] that solutions of the Navier–Stokes equations exhibit initial (in time) irregularity. Methods to deal with the lack of initial regularity are proposed in those references; see also the Annexe of Part 1 of Reference 14. Our concern here is *not* to consider this problem and thus in all that follows we shall set $t^0 = 0$ and assume that $\mathbf{u} \in L^\infty(0, T; H^{k+1}(\Omega))$, $\partial\mathbf{u}/\partial t \in L^2(0, T; H^k(\Omega))$ and $p \in L^2(0, T; H^{k'+1}(\Omega))$. We also assume that the regularity properties

$$\mathbf{u} \in L^\infty(0, T; W^{1,\infty}(\Omega)), \quad \frac{\partial^2\mathbf{u}}{\partial t^2} \in L^2(0, T; L^2(\Omega)), \quad \frac{\mathrm{d}^3\mathbf{g}_\mathbf{x}^{n+1}}{\mathrm{d}t^3} \in L^2(0, T; L^2(\Omega)) \tag{68}$$

hold, where $\mathbf{g}_\mathbf{x}^{n+1}$ is defined as in (37).

We derive from (51) the estimate for $1 \leqslant r \leqslant k+1$ and $1 \leqslant p \leqslant \infty$ as

$$\|\boldsymbol{\eta}\|_{L^p(0,T;L^2(\Omega))} + h\|\boldsymbol{\eta}\|_{L^p(0,T;H^1(\Omega))} \leqslant Ch^r\|\mathbf{u}\|_{L^p(0,T;H^r(\Omega))}. \tag{69}$$

Problem (60) is not completely defined, since it must be provided with the initial conditions $\mathbf{U}_h^0$ and $\mathbf{U}_h^1$. We assume for instance that they are initialized in such a way that

$$\boldsymbol{\xi}^0 = 0 \tag{70}$$

and $\mathbf{U}_h^1$ is an approximation of $\mathbf{u}^1$ such that

$$\frac{\|\boldsymbol{\xi}^1\|^2_{L^2(\Omega)}}{\Delta t} + \nu\|\nabla\boldsymbol{\xi}^1\|^2_{L^2(\Omega)} \leqslant K(h, \Delta t), \tag{71}$$

with

$$K(h, \Delta t) \leqslant C(\Delta t^4 + h^{2k} + h^{2(k'+1)}). \tag{72}$$

Here C indicates some positive constant independent of Δt and h.

4.2. A priori stability result

To prove the stability and convergence theorem, we need Lemma 4 and the following Lemma 5. We follow the framework of Ewing and Russell.[11] We denote by $C(.)$ any constant independent of Δt, h and n but depending on the set Ω and the variables in the brackets.

Let us define for any $t \in [t^{l-2}, t^l], 2 \leqslant l \leqslant N$, the following mapping on Ω:

$$\mathbf{x} \to \overline{\mathbf{X}}_{\mathbf{x}}^l(t) = \mathbf{x} - (t^l - t)\mathbf{U}_h^{(l-1)*}(\mathbf{x}). \tag{73}$$

Since X_h is a subset of $W^{1,\infty}(\Omega)$, under the sufficient condition

$$\Delta t < \frac{1}{2\|\mathbf{U}_h^{(l-1)*}\|_{W^{1,\infty}(\Omega)}} \tag{74}$$

on the time step it is an easy matter to verify that this mapping has a positive Jacobian, since $\mathbf{U}_h^{l*}$ vanishes on $\partial\Omega$; this mapping is one-to-one and thus it is a change of variables from Ω onto Ω (see References 21 and 14 for the two- and three-dimensional cases respectively). This yields for any positive functions φ on Ω the estimate

$$\int_\Omega \varphi\left(\overline{\mathbf{X}}_{\mathbf{x}}^l(t)\right)\mathrm{d}\mathbf{x} \leqslant C\int_\Omega \varphi(\mathbf{x})\mathrm{d}\mathbf{x}, \tag{75}$$

where the constant C is independent of l. We are thus led to introduce a uniform condition on Δt with respect to $1 \leqslant l \leqslant N-1$ and assume that

$$\Delta t < \frac{1}{2L_n}, \tag{76}$$

where

$$L_n = \max_{1 \leqslant l \leqslant n} \|\mathbf{U}_h^{l*}\|_{W^{1,\infty}(\Omega)}. \tag{77}$$

The condition (76) allows us to verify the property (74) for any l, $2 \leqslant l \leqslant n+1$. We denote also

$$M_n = \max_{1 \leqslant l \leqslant n} \|\mathbf{U}_h^{l*}\|_{L^\infty(\Omega)}. \tag{78}$$

From Lemmas 6–9 stated and proven in the Appendix, we can prove, also in the Appendix, the following Lemma.

Lemma 5

Let us assume that for any n, $1 \leqslant n \leqslant N-1$,

$$\Delta t < \frac{1}{2L_n}; \tag{79}$$

we have

$$|\mathbf{U}_h^{n+1} - \mathbf{w}_h^{n+1}|_{H^1(\Omega)} \leqslant C(M_n, \mathbf{u}, p, T, 1/\nu)(\Delta t^2 + h^k + h^{k'+1}), \tag{80}$$

where $C(M_n, \mathbf{u}, p, T, 1/\nu)$ blows up (exponentially) when ν tends to 0 or T tends to ∞.

The result of Lemma 5 gives an error estimate at each time step. We note that the constants in the error approximation (80) and in the condition (79) depend on n through M_n and L_n respectively. The aim of the next subsection is to give an error approximation independent of n.

4.3. Stability and convergence results

4.3.1. Stability and error estimate for velocity. From a bootstrapping argument we are able to derive from Lemma 51 the H^1 stability and establish convergence properties. This is given in the next theorem, which provides an optimal error bound.

Theorem 1

There exists constants C_1, C_2, C_3 and C_4 independent of h and Δt such that for h sufficiently small the condition

$$\Delta t \leqslant C_1 h^{d/6} \tag{81}$$

yields for all n, $0 \leqslant n \leqslant N$,

$$\|\mathbf{U}_h^n\|_{H^1(\Omega)} \leqslant C_2, \qquad \|\mathbf{U}_h^n\|_{L^\infty(\Omega)} \leqslant C_3 \tag{82}$$

$$\|\mathbf{u}(.,t^n) - \mathbf{U}_h^n\|_{H^1(\Omega)} \leqslant C_4(\Delta t^2 + h^k + h^{k'+1}). \tag{83}$$

Before giving the proof of this theorem, we describe the behaviour of the constants C_1, C_2, C_3 and C_4 in the following remark.

Remark 5

C_2 and C_3 depend only on the initial values $\mathbf{U}_h^0$ and $\mathbf{U}_h^1$ and the solution $\mathbf{u}$ of the problem (1)–(3). More precisely, we have

$$C_2 = \max\{\|\mathbf{U}_h^0\|_{H^1(\Omega)}, \|\mathbf{U}_h^1\|_{H^1(\Omega)}, 2\|\mathbf{w}_h\|_{L^\infty(0,T;H^1(\Omega))}\}, \tag{84}$$

$$C_3 = \max\{\|\mathbf{U}_h^0\|_{L^\infty(\Omega)}, \|\mathbf{U}_h^1\|_{L^\infty(\Omega)}, 2\|\mathbf{w}_h\|_{L^\infty(0,T;L^\infty(\Omega))}\}, \tag{85}$$

where we recall that

$$\mathbf{w}_h(t,.) = \Pi_{1,h}^0 \mathbf{u}(t,.).$$

The constants C_2 and C_3 are independent of h thanks to (51) and (53). The constants C_1^{-1} and C_4 depend not only on the initial values $\mathbf{U}_h^0$ and $\mathbf{U}_h^1$ and the solution $(\mathbf{u}, p)$ of the continuous problem (1)–(3) but also on the final time T and the viscosity coefficient ν. Moreover, they blow up when ν tends to 0 or when T tends to ∞. This means that this theorem is not yet proved in the steady state case. For the case $\nu \to 0$ it is treated by Boukir *et al.*,[1] who obtain stability results independent of ν.

Proof of Theorem 1

Thanks to (52), we choose C_5 such that

$$\max\left\{\frac{\|\mathbf{U}_h^0\|_{W^{1,\infty}(\Omega)}}{2}, \frac{\|\mathbf{U}_h^1\|_{W^{1,\infty}(\Omega)}}{2}, \|\mathbf{w}_h\|_{L^\infty(0,T;W^{1,\infty}(\Omega))}\right\} \leqslant \frac{C_5}{2} h^{-d/6}. \tag{86}$$

To show (82), we proceed by induction. Let us denote $\mathrm{P}(\mathbf{U}_h^l)$ as the property

$$\mathrm{P}(\mathbf{U}_h^l) \iff \begin{cases} \|\mathbf{U}_h^l\|_{H^1(\Omega)} \leqslant C_2, & (87) \\ \|\mathbf{U}_h^l\|_{L^\infty(\Omega)} \leqslant C_3, & (88) \\ \|\mathbf{U}_h^l\|_{W^{1,\infty}(\Omega} \leqslant C_5 h^{-d/6}, & (89) \end{cases}$$

where the constants C_2, C_3 and C_5 are those defined in (84)–(86). From (84)–(86) we deduce that $\mathrm{P}(\mathbf{U}_h^0)$ and $\mathrm{P}(\mathbf{U}_h^1)$ are true. Let us assume that $\mathrm{P}(\mathbf{U}_h^l)$ is true for all $2 \leqslant l \leqslant n$ (induction hypothesis); we

shall prove that $P(U_h^{n+1})$ is true. We have from the induction hypothesis and the definitions (77) and (78)

$$M_n \leqslant 3C_3, \tag{90}$$

$$L_n \leqslant 3C_5 h^{-d/6}. \tag{91}$$

For a proper choice of C_1 ($C_1 < 1/6C_5$) the conditions (81) and (91) allow us to fulfil the hypothesis (79). From Lemma 5, since $k' < k$, this leads to

$$\|U_h^{n+1} - w_h^{n+1}\|_{H^1(\Omega)} \leqslant C(C_3)(h^{k'+1} + \Delta t^2). \tag{92}$$

Using the triangular inequality, we get

$$\|U_h^{n+1}\|_{H^1(\Omega)} \leqslant \|U_h^{n+1} - w_h^{n+1}\|_{H^1(\Omega)} + \|w_h^{n+1}\|_{H^1(\Omega)}.$$

It follows from (84) and (92) that

$$\|U_h^{n+1}\|_{H^1(\Omega)} \leqslant C(C_3)(h^{k'+1} + \Delta t^2) + \frac{C_2}{2}. \tag{93}$$

For h sufficiently small and owing to (81), we obtain the property (87) for $l = n+1$. To show (88), we first use the triangular inequality

$$\|U_h^{n+1}\|_{L^\infty(\Omega)} \leqslant \|U_h^{n+1} - w_h^{n+1}\|_{L^\infty(\Omega)} + \|w_h^{n+1}\|_{L^\infty(\Omega)}.$$

Using the inverse inequality $\|v_h\|_{L^\infty(\Omega)} \leqslant C \log(1/h)\|v_h\|_{H^1(\Omega)}$ in 2D[18] or $\|v_h\|_{L^\infty(\Omega)} \leqslant C(1/\sqrt{h})\|v_h\|_{H^1(\Omega)}$ in 3D,[18] we have

$$\|U_h^{n+1}\|_{L^\infty(\Omega)} \leqslant \begin{cases} C \log\left(\frac{1}{h}\right)\|U_h^{n+1} - w_h^{n+1}\|_{H^1(\Omega)} + \|w_h^{n+1}\|_{L^\infty(\Omega)} & \text{in 2D,} \\ C\frac{1}{\sqrt{h}}\|U_h^{n+1} - w_h^{n+1}\|_{H^1(\Omega)} + \|w_h^{n+1}\|_{L^\infty(\Omega)} & \text{in 3D.} \end{cases} \tag{94}$$

It follows from (85) and (92) that

$$\|U_h^{n+1}\|_{L^\infty(\Omega)} \leqslant \begin{cases} \log\left(\frac{1}{h}\right)C(C_3)(h^{k'+1} + \Delta t^2) + \frac{C_3}{2} & \text{in 2D,} \\ \frac{1}{\sqrt{h}}C(C_3)(h^{k'+1} + \Delta t^2) + \frac{C_3}{2} & \text{in 3D.} \end{cases} \tag{95}$$

For h sufficiently small and with the condition (81) the property (88) for $l = n+1$ is deduced from (95). To show (89), we first use the triangular inequality

$$\|U_h^{n+1}\|_{W^{1,\infty}(\Omega)} \leqslant \|U_h^{n+1} - w_h^{n+1}\|_{W^{1,\infty}(\Omega)} + \|w_h^{n+1}\|_{W^{1,\infty}(\Omega)}.$$

Thanks to the inverse inequality $\|v_h\|_{W^{1,\infty}(\Omega)} \leqslant Ch^{-d/2}\|v_h\|_{H^1(\Omega)}$,[18] we get

$$\|U_h^{n+1}\|_{W^{1,\infty}(\Omega)} \leqslant Ch^{-d/2}\|U_h^{n+1} - w_h^{n+1}\|_{H^1(\Omega)} + \|w_h^{n+1}\|_{W^{1,\infty}(\Omega)}. \tag{96}$$

It follows from (92) and (86) that

$$\begin{aligned} \|U_h^{n+1}\|_{W^{1,\infty}(\Omega)} &\leqslant h^{-d/2}C(C_3)(h^{k'+1} + \Delta t^2) + \frac{C_5}{2}h^{-d/6} \\ &\leqslant h^{-d/6}C(C_3)(h^{k'+1-d/3} + \Delta t^2 h^{-d/3}) + \frac{C_5}{2}h^{-d/6}. \end{aligned} \tag{97}$$

Then the result (89) with $l=n+1$ follows from the condition (81), a proper choice of C_1 (i.e. sufficiently small to satisfy in addition the inequality $C_1^2 C(C_3) \leqslant C_5/4$) and the hypothesis that h is sufficiently small in the case $k'+1-d/3>0$. If $k'+1-d/3=0$, we get the same result by slightly modifying the proof (choose a bigger C_5). This finishes the proof of the stability result (82).

Using the result (89) and the condition (81) on Δt with $C_1 < 1/6C_5$, we can apply Lemma 5, and combined with the estimate (82), we get the result (83).

Remark 6. The case $\operatorname{div} \mathbf{U}_h^{n*} = 0$

When the characteristics are transported by a divergence-free velocity[5] and assumed to be exactly computed, instead of the mapping defined in (73), we use the transformation $\mathbf{y} = \mathbf{X}_{\mathbf{x}}^l(t)$, where $\mathbf{X}_{\mathbf{x}}^l(t)$ is defined as in (17). From Liouville's identity the Jacobian of this mapping satisfies

$$J(t) = \exp\left(\int_{t^l}^{t} \nabla \cdot \mathbf{U}_h^{(l-1)*}(\mathbf{X}_{\mathbf{x}}^l(t))\mathrm{d}t\right) = 1. \tag{98}$$

The condition (74) can be omitted in the previous investigations. Thus in the proof of the theorem we do not need the inverse inequality which fixes the norms $\|.\|_{W^{1,\infty}(\Omega)}$ and $\|.\|_{H^1(\Omega)}$. Only the inequality which fixes the norms $\|.\|_{L^\infty(\Omega)}$ and $\|.\|_{H^1(\Omega)}$ is used. This leads to the following corollary.

Corollary 1

There exist constants C_1', C_2', C_3' and C_4' independent of h and Δt such that for h sufficiently small the conditions

$$\nabla \cdot \mathbf{U}_h^{n*} = 0,$$
$$\Delta t \leqslant \frac{C_1'}{\log(1/h)} \quad (\text{in 2D}), \qquad \Delta t \leqslant C_1' h^{1/4} \quad (\text{in 3D}) \tag{99}$$

yield for all n, $0 \leqslant n \leqslant N$,

$$\|\mathbf{U}_h^n\|_{H^1(\Omega)} \leqslant C_2', \qquad \|\mathbf{U}_h^n\|_{L^\infty(\Omega)} \leqslant C_3', \tag{100}$$

$$\|\mathbf{u}(.,t^n) - \mathbf{U}_h^n\|_{H^1(\Omega)} \leqslant C_4'(\Delta t^2 + h^k + h^{k'+1}), \tag{101}$$

where the constants C_1', C_2', C_3' and C_4' have the same behaviour as the constants C_1, C_2, C_3 and C_4 of Theorem 1.

4.3.2. Error estimate for pressure. The following result on the pressure is a consequence of the previous results on the velocity.

Theorem 2

There exists a constant C independent of h and Δt but dependent on $\mathbf{u}$, p, T and $1/\nu$ such that the condition (81) yields

$$\left(\sum_{l=0}^{N} \Delta t \|p^l - P_h^l\|_{L^2(\Omega)}^2\right)^{1/2} \leqslant C(\Delta t^2 + h^k + h^{k'+1}). \tag{102}$$

Proof. Let us introduce the element $\Pi_h' p^l$ of the space Q_h; we have from the triangle inequality

$$\|p^l - P_h^l\|_{L^2(\Omega)} \leqslant \|p^l - \Pi_h' p^l\|_{L^2(\Omega)} + \|\Pi_h' p^l - P_h^l\|_{L^2(\Omega)}. \tag{103}$$

Since $\Pi'_h p^l - P_h^l$ is in Q_h, it follows from the inf-sup condition (48) that

$$\|\Pi'_h p^l - P_h^l\|_{L^2(\Omega)} \leqslant C \sup_{\mathbf{v}_h \in X_h} \frac{(\nabla \cdot \mathbf{v}_h, \Pi'_h p^l - P_h^l)}{\|\mathbf{v}_h\|_{H^1(\Omega)}}.$$

Multiplying the consistency error (117) (see Appendix) by $\mathbf{v}_h \in X_h$ and subtracting the resulting expression from (60), we obtain

$$\begin{aligned}(\nabla \cdot \mathbf{v}_h, \Pi'_h p^l - P_h^l) = &- (\underline{\mathbf{e}}(., l), \mathbf{v})_h) + \left(\frac{4(\bar{\mathbf{u}}^{l-1} - \underline{\mathbf{u}}^{l-1}) - (\bar{\bar{\mathbf{u}}}^{l-2} - \underline{\bar{\mathbf{u}}}^{l-2})}{2\Delta t}, \mathbf{v}_h\right) \\ &+ \left(\frac{3\eta^l - 4\bar{\eta}^{l-1} + \bar{\bar{\eta}}^{l-2}}{2\Delta t}, \mathbf{v}_h\right) + \left(\frac{4(\bar{\boldsymbol{\xi}}^{l-1} - \boldsymbol{\xi}^{l-1}) - (\bar{\bar{\boldsymbol{\xi}}}^{l-2} - \boldsymbol{\xi}^{l-2})}{2\Delta t}, \mathbf{v}_h\right) \\ &- \left(\frac{3\boldsymbol{\xi}^l - 4\boldsymbol{\xi}^{l-1} + \boldsymbol{\xi}^{l-2}}{2\Delta t}, \mathbf{v}_h\right) + \nu(\nabla(\mathbf{u}^l - \mathbf{U}_h^l), \nabla \mathbf{v}_h) + (\nabla \cdot \mathbf{v}_h, \Pi'_h p^l - p^l).\end{aligned}$$

Using the Cauchy–Schwarz inequality, we have

$$\|\Pi'_h p^l - P_h^l\|_{L^2(\Omega)} \leqslant \sum_{i=1}^{4} \|\mathbf{F}_i^l\|_{L^2(\Omega)} + \left\|\frac{3\delta\boldsymbol{\xi}^l - \delta\boldsymbol{\xi}^{l-1}}{2\Delta t}\right\|_{L^2(\Omega)} + \nu|\mathbf{U}_h^l - \mathbf{u}^l|_{H^1(\Omega)} + \|\Pi'_h p^l - p^l\|_{L^2(\Omega)}, \quad (104)$$

where the terms $\mathbf{F}_i^l$ are those defined in (117), (119), (123) and (134) (see Appendix). Summing (104) from $l=2$ to N, we obtain from (103)

$$\begin{aligned}\sum_{l=2}^{N} \Delta t \|P_h^l - p^l\|_{L^2(\Omega)}^2 \leqslant C\Bigg(&\sum_{l=2}^{N} \Delta t \|\Pi'_h p^l - p^l\|_{L^2(\Omega)}^2 + \sum_{i=1}^{4} \sum_{l=2}^{N} \Delta t \|\mathbf{F}_i^l\|_{L^2(\Omega)}^2 \\ &+ \nu \sum_{l=2}^{N} \Delta t |\mathbf{U}_h^l - \mathbf{u}^l|_{H^2(\Omega)}^2 + \sum_{l=1}^{N} \frac{1}{\Delta t} \|\delta\boldsymbol{\xi}^l\|_{L^2(\Omega)}^2\Bigg). \quad (105)\end{aligned}$$

To handle the last term on the right-hand side of (105), we refer to the estimate (146) (see Appendix), which leads to

$$\sum_{l=2}^{n+1} \frac{\|\delta\boldsymbol{\xi}^l\|_{L^2(\Omega)}^2}{\Delta t} \leqslant \sum_{i=1}^{4} \sum_{l=2}^{n+1} \mathbf{F}_i^l(\delta\boldsymbol{\xi}^l) + \sum_{l=2}^{n+1} \mathbf{F}_5^l(\delta\boldsymbol{\xi}^l) + K(h, \Delta t), \quad (106)$$

which from the inequality $2ab \leqslant a^2 + b^2$ leads to

$$\sum_{l=2}^{n+1} \frac{\|\delta\boldsymbol{\xi}^l\|_{L^2(\Omega)}^2}{\Delta t} \leqslant C \sum_{i=1}^{4} \sum_{l=2}^{n+1} \Delta t \|\mathbf{F}_i^l\|_{L^2(\Omega)}^2 + \frac{1}{2} \sum_{l=2}^{n+1} \frac{\|\delta\boldsymbol{\xi}^l\|_{L^2(\Omega)}^2}{\Delta t} + \sum_{l=2}^{n+1} \mathbf{F}_5^l(\delta\boldsymbol{\xi}^l) + K(h, \Delta t). \quad (107)$$

The result (102) is then deduced from (105), (55), Lemmas 6–9 (see Appendix) and Theorem 1.

5. NUMERICAL RESULTS; COMPARISON WITH FIRST-ORDER TIME SCHEME USING CHARACTERISTICS

In this section we present numerical results obtained with the N3S code developed at Electricité de France.[10]

The first numerical example deals with a steady case that has an analytical solution. Though the current theoretical results are valid only for unsteady computations (i.e. the solution is computed for

$n\Delta t \leqslant T$), we can observe that the difference between the numerical steady state velocity and the exact solution still behaves as expected from Theorem 1 (for the computation of a steady state the solution is the limit of the sequence $(\mathbf{U}_h^n)_n$). Stability for steady computations is investigated in Reference 14. We also provide numerical results on the pressure accuracy. For the second example an unsteady case is treated where the transient state is studied. In both cases the second-order scheme is compared with a first-order scheme[4,5] defined as follows. The convection step is solved by computing for $\mathbf{x} \in \Omega$ the characteristic curve

$$\mathbf{X}_{\mathbf{x}}^{n+1}: [t^n, t^{n+1}] \to \mathbb{R}^d,$$

the solution of

$$\begin{aligned} \frac{d\mathbf{X}_{\mathbf{x}}^{n+1}}{dt} &= \mathbf{U}^n(\mathbf{X}_{\mathbf{x}}^{n+1}(t)) \quad \text{in } [t^n, t^{n+1}[, \\ \mathbf{X}_{\mathbf{x}}^{n+1}(t^{n+1}) &= \mathbf{x}. \end{aligned} \tag{108}$$

We set

$$\tilde{\mathbf{U}}^n(\mathbf{x}) = \mathbf{U}^n(\mathbf{X}_{\mathbf{x}}^{n+1}(t^n)). \tag{109}$$

Then we solve a Stokes problem by computing $\mathbf{U}^{n+1}: \Omega \to \mathbb{R}^d$ and $P^{n+1}: \Omega \to \mathbb{R}$, the solution of

$$\begin{aligned} \frac{\mathbf{U}^{n+1} - \tilde{\mathbf{U}}^n}{\Delta t} - \nu \Delta \mathbf{U}^{n+1} + \nabla P^{n+1} &= \mathbf{f}^{n+1} \quad \text{in } \Omega, \\ \operatorname{div} \mathbf{U}^{n+1} &= 0 \quad \text{in } \Omega, \\ \mathbf{U}^{n+1} &= \mathbf{u}_d^{n+1} \quad \text{over } \partial\Omega. \end{aligned} \tag{110}$$

The numerical results show clearly the improvements given by the second-order scheme.

Remark 7

The scheme that has actually been implemented is based on the following approach.

(i) For the first- (resp. second-) order scheme the characteristic curves are computed with the help of a first- (resp. second-) order Runge–Kutta scheme together with a multistep procedure in the first example (see (40) (resp. (43) and (44)). In the second example, in the case of the second-order scheme the characteristic curves are computed with the help of the multistep first-order scheme (40). Note that in the case of the second-order scheme the results are the same with the second-order Runge–Kutta scheme (43), (44) or the scheme (40).

(ii) As regards the fully discrete scheme (58)–(60), in the computations, for the sake of simplicity, the quantities $\overline{\mathbf{U}}_h^n$ and $\overline{\overline{\mathbf{U}}}_h^{n-1}$ are replaced by $I_h\overline{\mathbf{U}}_h^n$ and $I_h\overline{\overline{\mathbf{U}}}_h^{n-1}$, where I_h is the interpolation operator at the velocity nodes. An analogous approximation is performed for the first-order scheme. This is not taken into account in the previous theoretical analysis. Nevertheless, estimates similar to (83) and (102) are observed numerically. However, conditional instability has been noticed:[22] the scheme blows up when the time step is too small. Such a behaviour has already been observed in References 15 and 16, where the stability in the case of non-exact integration is treated for the first-order scheme. Referring to those papers, we can suspect the interpolation operator of polluting the stability of the scheme. A similar conclusion is given in Reference 14.

(iii) Note also that in the first case computations are realized for the non-homogeneous Dirichlet boundary condition problem.

Remark 8

Concerning the difference in computation costs between the two schemes, the second-order scheme is more expensive than the first-order one because its convection step is twice as long. Nevertheless, this is not very penalizing, since generally the convection step is much cheaper than the Stokes step. In our code, where the Stokes step is solved with the help of a Uzawa method using a preconditioned conjugate gradient algorithm on the pressure,[10] the ratio is about 1:10.

5.1. Numerical results for a steady analytical case: a vortex in a square cavity

Here we have $\Omega =]0, 1[\times]-\frac{1}{2}, \frac{1}{2}[$; for a given parameter b we set

$$\nu = 1/b. \tag{111}$$

The body forces are equal to

$$\mathbf{f} = \begin{bmatrix} \pi b^2 \cos(\pi x)\sin(\pi x) \\ -\pi b^2 \sin(\pi y)\cos(\pi y) + 4\pi^2 \cos(\pi y)\cos(\pi y) \end{bmatrix} \tag{112}$$

and the boundary conditions are

$$\begin{aligned} u_x(0, y) &= 0, & u_y(0, y) &= \cos(\pi y), \\ u_x(1, y)0, & & u_y(1, y) &= -b\cos(\pi y), \\ u_x(x, -\tfrac{1}{2}) &= -b\sin(\pi x), & u_y(x, -\tfrac{1}{2}) &= 0, \\ u_x(x, \tfrac{1}{2}) &= b\sin(\pi x), & u_y(x, \tfrac{1}{2}) &= 0. \end{aligned}$$

In this case we can verify that the problem (1), (2) has the (steady) analytical solution

$$\begin{aligned} u_x(x, y) &= b\sin(\pi x)\sin(\pi y), \\ u_y(x, y) &= b\cos(\pi x)\cos(\pi y), \\ p(x, y) &= 2\pi\cos(\pi x)\sin(\pi y). \end{aligned} \tag{113}$$

Note that the solution verifies on Ω

$$\begin{aligned} -b \leqslant u_x \leqslant b, \qquad -b \leqslant u_y \leqslant b, \\ \|\mathbf{u}\|_{L^\infty} = b, \\ \Delta p = p_{\max} - p_{\min} = 4\pi = 12{\cdot}57. \end{aligned} \tag{114}$$

The numerical results are given here for $b = 10$. The solution (113) is presented in Figure 1.

5.1.1. Behaviour according to time step. We first compare the results obtained by the first- and second-order schemes for three different time steps (see Figures 2 and 3, where on the left are represented the iso-U_x lines and on the right the iso-pressure lines). The computations are realized with the triangular finite element P_2–P_1, the mesh is regular and the number of velocity nodes is equal to 43 in eace space direction.

To compare the two schemes, we can say that although the velocity is more precisely computed than the pressure for a given time step, its behaviour changes with the scheme near the boundaries $y = -\frac{1}{2}$ and $y = \frac{1}{2}$. However, in all cases its global order of magnitude is good. This is not the case for the

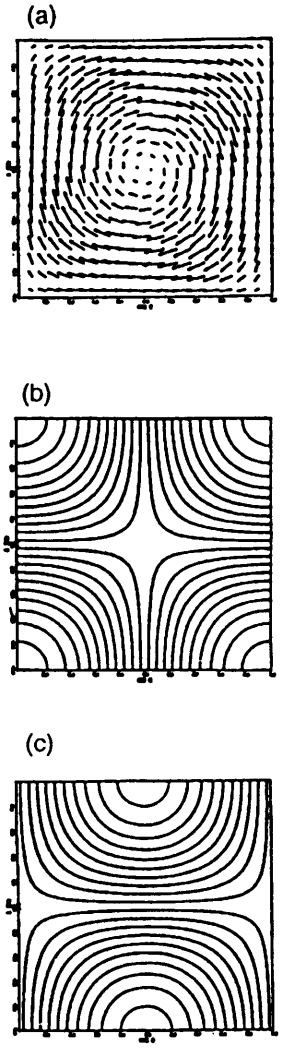

Figure 1. Vortex in a cavity—analytical solution: (a) iso-u_x lines; (b) iso-pressure lines; (c) velocity field

pressure, which is why we have indicated on Figures 2 and 3 for each case the difference between the maximum and minimum of its computed value ΔP (to compare with (114)).

Thus, when comparing Figures 1–3, we observe that for each scheme the results are improved when the time step is decaying. Moreover, it is obvious that for each time step the results are better for the second-order scheme. We also notice that the results obtained by the first-order scheme at the time step $\Delta t = 2 \times 10^{-4}$ are qualitatively similar to those obtained with the second-order one for $\Delta t = 10^{-2}$. (Note also that for $\Delta t = 10^{-4}$ the first-order scheme does not converge; this numerical instability is probably due to the fact that the time step is too small compared with the space one, which is not the case for the second-order scheme.)

We also obtain an evaluation of the time accuracy orders by plotting the relative discrete $l^{\infty}(\Omega)$ error as a function of the time step (see Figure 4).

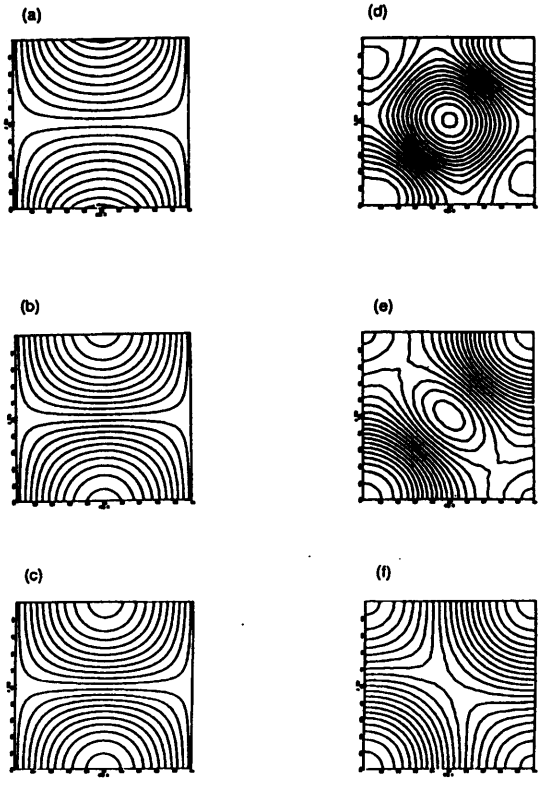

Figure 2. Vortex in a cavity—first-order scheme: iso-U_x lines ((a) $\Delta t = 10^{-2}$; (b) $\Delta t = 10^{-3}$; (c) $\Delta t = 2 \times 10^{-4}$); iso-pressure lines ((d) $\Delta t = 10^{-2}$, $\Delta P = 42{\cdot}30$; (e) $\Delta t = 10^{-3}$, $\Delta P = 13{\cdot}45$; (f) $\Delta t = 2 \times 10^{-4}$, $\Delta P = 12{\cdot}60$)

For these computations we have used a regular 81 × 81 velocity mesh. When using logarithmic scales, the obtained curves are almost straight lines, the slopes of which represents the time order. The slopes for the first-order scheme are equal to 1·12 and 1·23 for the velocity and pressure respectively, in agreement with the results obtained by Pironneau[5] and Suli.[7] For the second-order scheme the slope is 1·97 for both the velocity and the pressure, in agreement with the results of Theorems 1 and 2. Notice also that according to Figure 4 the second-order scheme is quantitatively more accurate than the first-order one. For instance, the corresponding velocity errors are almost the same with the second-order scheme for the time step 10^{-3} (resp. 10^{-2}) and with the first-order scheme for the time step 2×10^{-5} (resp. 7×10^{-4}). We also obtain the same pressure errors for the time step 10^{-3} (resp. 10^{-2}) with the second-order scheme and for the time step 10^{-5} (resp. 3×10^{-4}) with the first-order scheme.

5.1.2. Behaviour according to space step. Here only the second-order scheme is studied, the time step is fixed ($\Delta t = 10^{-5}$) and we study the variation in the discrete $l^2(\Omega)$ relative error of the velocity as a function of the space step. Still with logarithmic scales, the obtained curve is almost a straight line, the slope of which represents the space accuracy order s relative to the $l^2(\Omega)$ norm (see Figure 5). Assume that the finite element is P_k–$P_{k'}$. We can then deduce that the numerical accuracy H^1 order k_{num} of the velocity is greater than $\min(k, k'+1, s-1)$. For the finite element P_2–P_1 we obtain $s = 3{\cdot}2$, so $k_{\text{num}} \geqslant 2$. For the finite element P_1–iso-P_1, for which the pressure is P_1 on each triangle and the velocity is P_1 on four subtriangles obtained by joining the middle points of the edges, we obtain $s = 2$, so $k_{\text{num}} \geqslant 1$. Note that these results obtained for the steady case are in good agreement with the result (83) which treats the unsteady case.

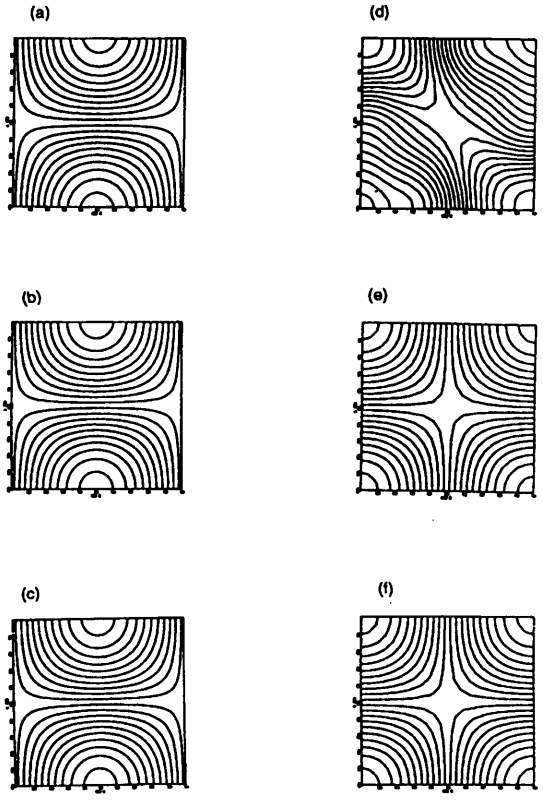

Figure 3. Vortex in a cavity–second-order scheme: iso-U_x lines ((a) $\Delta t = 10^{-2}$; (b) $\Delta t = 10^{-3}$; (c) $\Delta t = 10^{-4}$); iso-pressure lines ((d) $\Delta t = 10^{-2}$, $\Delta P = 12{\cdot}62$; (e) $\Delta t = 10^{-3}$, $\Delta P = 12{\cdot}60$; (f) $\Delta t = 10^{-4}$, $\Delta P = 12{\cdot}60$)

5.2. Numerical results for an unsteady case: natural convection in a rectangular cavity

The case presented here has been studied during a GAMM workshop.[23] We treat the laminar flow of an incompressible fluid in a rectangular cavity with an aspect ratio of 4 (the length L and height H are equal to 4 and 1 respectively), the vertical walls of which are heated at two different temperatures θ_1 and θ_2 (see Figure 6). We can assume that the Boussinesq approximation is applicable. Moreover, we consider the limit case where the Prandtl number Pr is equal to zero. In this case, by adimensionalizing the equations, we obtain that

(i) the temperature θ can be expressed analytically as $\theta = x$
(ii) it only remains to solve the coupled velocity–pressure Navier–Stokes equations

$$\frac{\partial \mathbf{u}}{\partial t} - \nu \Delta \mathbf{u} + \mathbf{u} \cdot \nabla \mathbf{u} + \operatorname{grad} p = -Gr \frac{x}{H} \mathbf{j} \quad \text{in } \Omega \times]0, T[, \tag{115}$$

$$\operatorname{div} \mathbf{u} = 0 \quad \text{in } \Omega \times]0, T[, \tag{116}$$

where $\mathbf{j}$ is the vertical unit vector and Gr is the Grashoff number.

One of the aims of the workshop was to study the behaviour of the flow according to the Grashoff number value. According to the guidelines, the computations were to be done successively for several values of Gr: $Gr = 20{,}000$, 25,000, 30,000 and 40,000. The initial velocity was advised to be taken

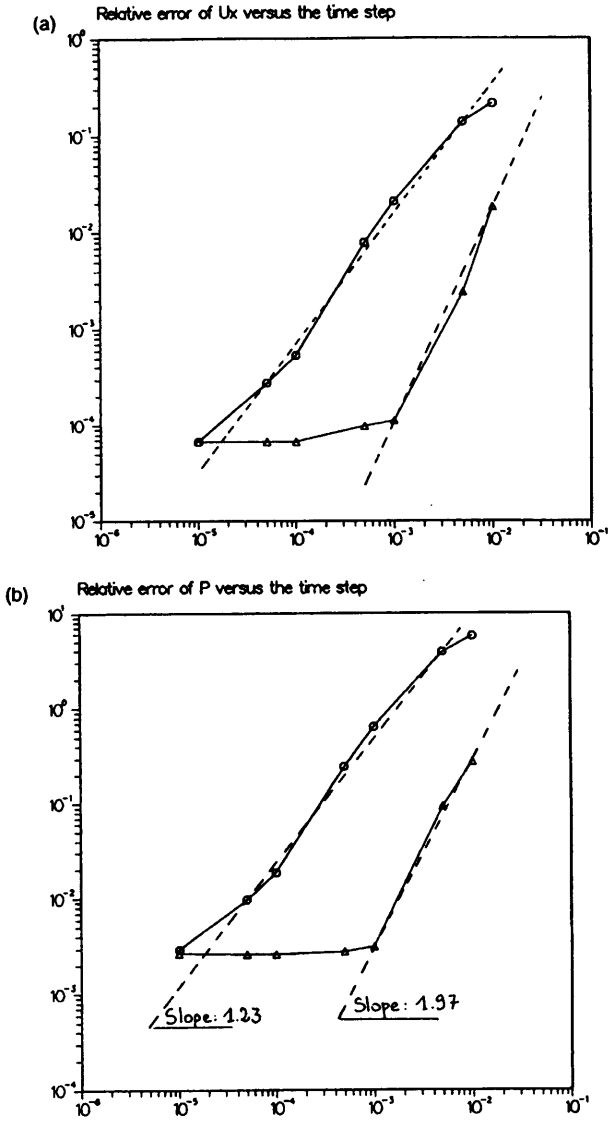

Figure 4. Vortex in a cavity (81 × 81 velocity mesh)—relative discrete $l^{\infty}(\Omega)$ error as a function of time step: (a) velocity component U_x; (b) pressure; O, first-order scheme; Δ, second-order scheme

equal to zero for $Gr = 20{,}000$ and to the velocity obtained by the previous computation for the other values of Gr. Our computations have been realized on a regular 97 × 41 velocity node mesh and with the P_1–iso-P_1 finite element. Note that this very coarse mesh is used only to demonstrate the superiority of the second-order method and could be improved by refining the spatial discretization. The time step is equal to 10^{-4}. For the sake of brevity we will focus here on the results obtained for $Gr = 30{,}000$ and 40,000 (for more details see Reference 22). Figures 7–10 present the results obtained for both schemes. They show at five points A(0·75, 0·5), B(2, 0·19), C(2, 0·5), D(2, 0·81) and E(3·25, 0·5) the velocity component U_y as a function of time and the iso-values of the normalized streamfunction $\psi/Gr^{1/2}$ at a fixed time.

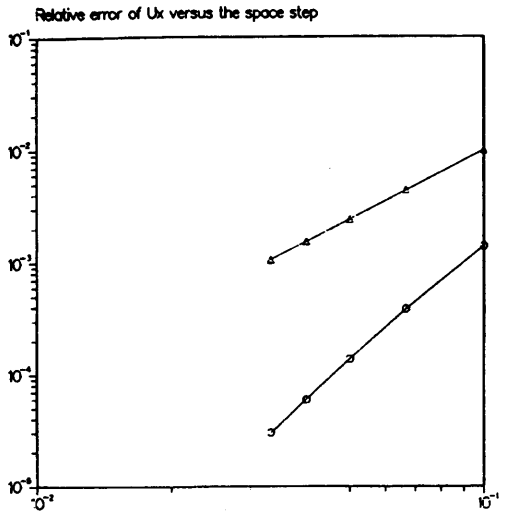

Figure 5. Vortex in a cavity (200 time steps, $\Delta t = 1 \times 10^{-5}$)—relative discrete $l^2(\Omega)$ error of velocity component U_x as a function of space step: O, P_2– P_1; Δ, P_1–iso-P_1

(i) For $Gr = 30{,}000$, according to the synthesis of the workshop,[23] the solution generally obtained by the contributors is monoperiodic with frequency $17{\cdot}4 < f < 17{\cdot}9$. The flow has a three-cell structure (one central main cell and two adjacent small cells). This structure is particularly clear at $t = t_0 + 0{\cdot}5P$, if where P is the period and t_0 is the instant when the maximum of $\max_y |U_x(1, y, t)|$ is reached. Note also that with very precise computations we can observe that the flow becomes quasiperiodic after a long time integration. Concerning our numerical results, the second-order scheme (see Figure 8) produces the periodic state with $f = 17{\cdot}54$. The amplitudes of U_x are equal to 0·3677 and 0·0315 for the second- and first-order schemes respectively! The second-order results are therefore very close to the best obtained in Reference 23, approximately 0·41. Still referring to Reference 23, we observe that the streamfunction has good features for the second-order scheme. However, this is not the case for the first-order scheme (see Figure 7): the computed state is periodic with a too large frequency $f = 18{\cdot}5$, the amplitude is too small and the three-cell structure is less sharp. Nevertheless, even with the second-order scheme we do not observe the quasiperiodic state, perhaps owing to a too short time integration interval (the computation has been realized in 6000 time steps).

(ii) For $Gr = 40{,}000$, according to the synthesis of the workshop,[23] the flow generally obtained exhibits very stable oscillations which persist for several tens of periods. The final solution is again centrosymmetric and is a two-cell structure. This structure appears with the second-order scheme (see Figure 10) when a steady state is reached, but only after about 12 periods (recall that our mesh is very coarse). However, this result is far better than that obtained with the first-order scheme. Indeed, with the latter we compute a periodic state with frequency $f = 21{\cdot}73$ and a three-cell structure for the

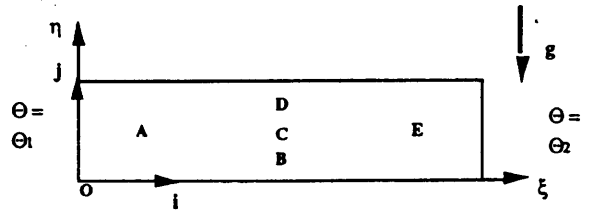

Figure 6. Natural convection in a rectangular cavity—computational domain

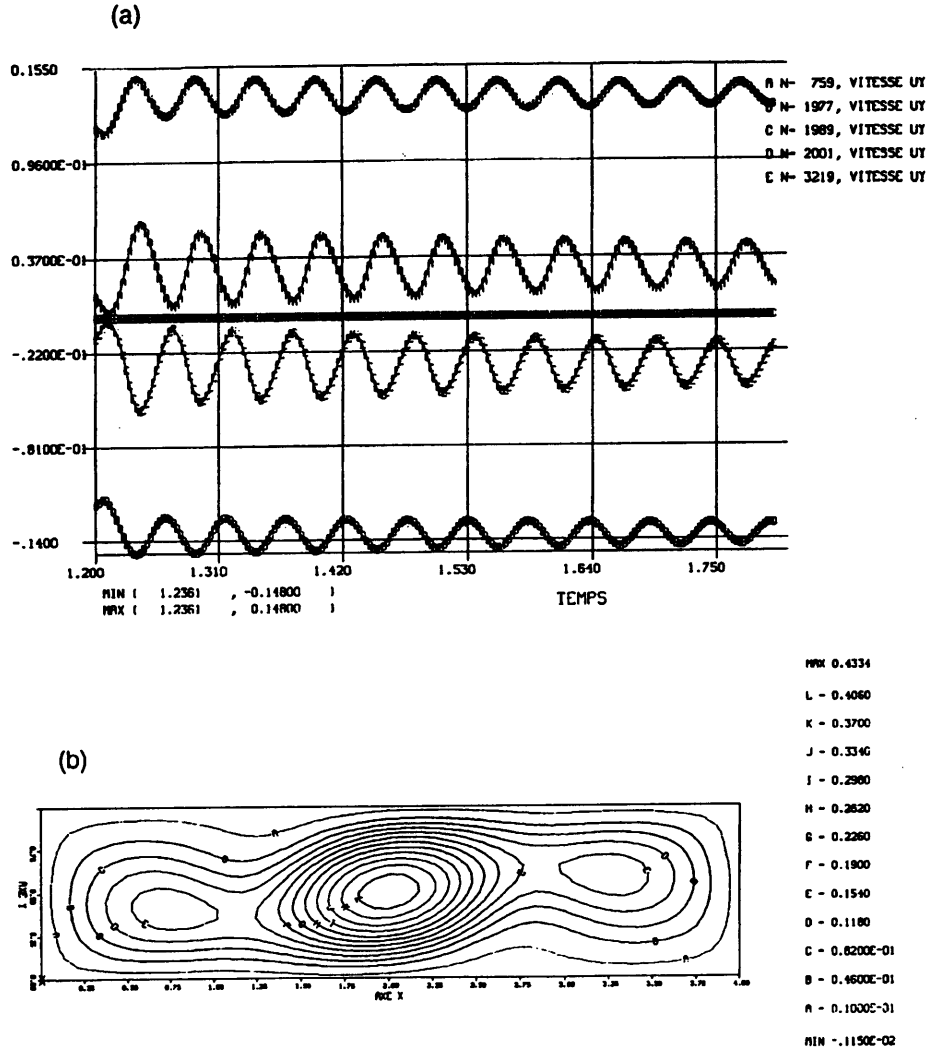

Figure 7. Natural convection in a rectangular cavity at $Pr = 0$, $Gr = 30{,}000$—first-order scheme: (a) U_y at points A–E as a function of time; (b) iso-values of streamfunction

streamfunction (see Figure 9). These results need to be sharpened by the use of a more refined approximation in space, so we do not show the plots, which are illustrated in References 14, 15 and 24.

6. CONCLUSIONS

We have presented an algorithm for the incompressible Navier–Stokes equations that uses a finite element method in space and a second-order Lagrangian time discretization. Second-order accuracy in time is achieved thanks to a backward differentiation approximation of the total derivative of the velocity. This method is an extension of the standard (first-order) method of characteristics.

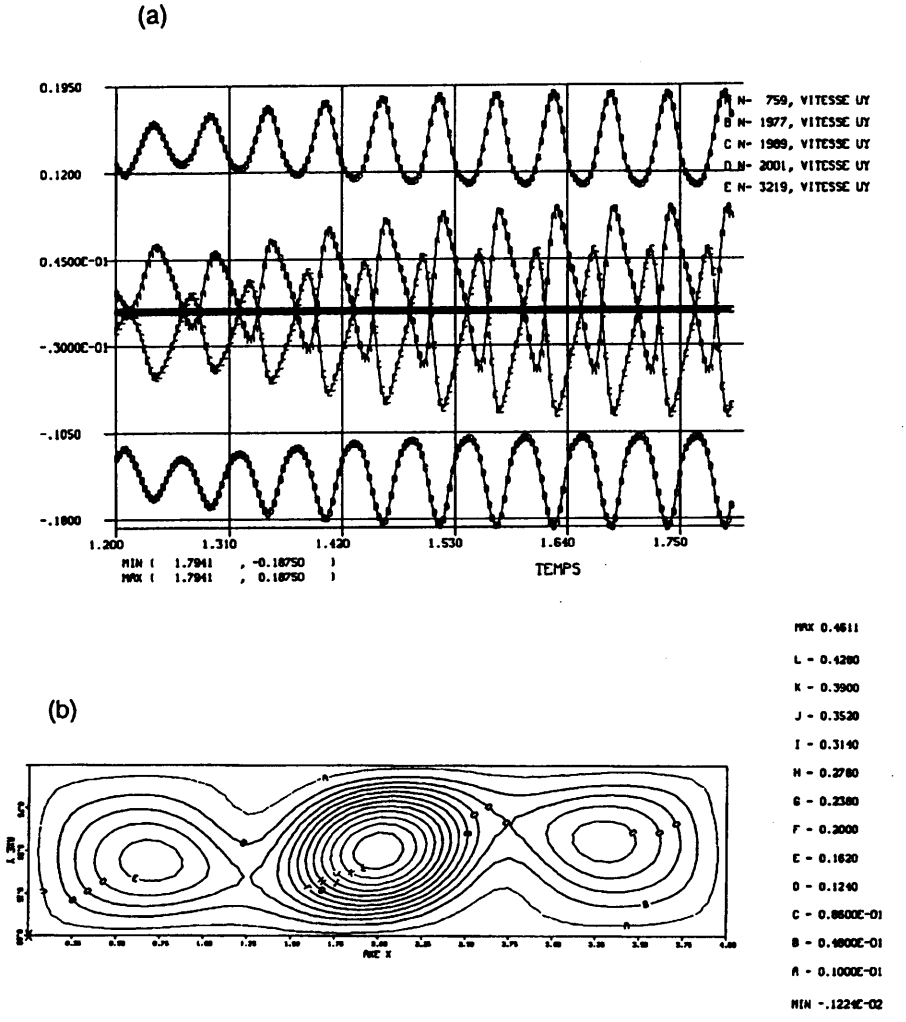

Figure 8. Natural convection in a rectangular cavity at $Pr=0$, $Gr=30{,}000$—second-order scheme: (a) U_y at points A–E as a function of time; (b) iso-values of streamfunction

The paper contains theoretical results concerning the H^1 stability of this scheme under a less stringent CFL condition than for the first-order scheme[7,14] in the case where the transport velocity is not exactly divergence-free. Optimal convergence results are also given for both velocity and pressure. The proof is based on a bootstrapping argument that involves

(i) an error estimate at each time step under the hypothesis that the numerical solution at the previous time steps is bounded
(ii) conditional stability derived from the error estimate under the assumption that the continuous solution is bounded.

This analysis is illustrated with numerical evidence showing that the second-order scheme is far superior to its first-order counterpart. Note that the extra cost of the second-order scheme only slightly

increases the cost of the computations (only the convection step is doubled with respect to the first-order scheme).

In this paper we do not address theoretically the effects of quadrature formulae related to the use of the interpolation operator on the convected fields. Note that the numerical results exhibit instabilities when the time step is too small with respect to the space step. This behaviour has already been observed for the first-order scheme in the literature.[15,16] We refer to Reference 14 for theoretical results in this direction. We also do not address theoretically the behaviour of this scheme either for long ranges of time or for a viscosity parameter tending to zero. The latter case is treated in Reference 1. Concerning the former case, however, note that the numerical simulation treats both steady and unsteady flows. A question that still needs to be considered is related to the drawback generally assigned to the characteristics method, i.e. the problem of lack of mass preservation. Although we have not noticed bad results in this direction for the experiments we did, the question needs further investigation.

If higher accuracy in time is required (e.g. owing to a more accurate discretization in space), we refer to Reference 22, where a kth-order version of this scheme is presented. The particular choice of third- and fourth-order schemes coupled with a spectral element spatial discretization has been presented in Reference 3 and theoretical proofs are given for the third-order scheme in References 1 and 14. The stability conditions are even weaker in this case than for the first- or second-order version. This adds even more interest to the high-order characteristics schemes.

APPENDIX

This appendix is devoted to the proof of Lemma 5.

For the sake of convenience let us set for $2 \leqslant l \leqslant N$

$$\mathbf{F}_1^l = -\underline{\mathbf{e}}(., l) = -\frac{3\mathbf{u}^l - 4\underline{\mathbf{u}}^{l-1} + \underline{\underline{\mathbf{u}}}^{l-2}}{2\Delta t} + \nu\Delta\mathbf{u}^l - \nabla p^l + \mathbf{f}^l. \tag{117}$$

Using the regularity hypothesis (68), we have from Lemma 4 for $n+1 \leqslant N$.

$$\sum_{l=2}^{n+1} \Delta t \|\mathbf{F}_1^l\|_{L^2(\Omega)}^2 \leqslant C(\mathbf{u}, T)\Delta t^4. \tag{118}$$

Lemma 6

We set for $2 \leqslant l \leqslant N$

$$\mathbf{F}_2^l = \frac{4(\overline{\mathbf{u}}^{l-1} - \underline{\mathbf{u}}^{l-1}) - \left(\overline{\overline{\mathbf{u}}}^{l-2} - \underline{\underline{\mathbf{u}}}^{l-2}\right)}{2\Delta t}. \tag{119}$$

We have

$$\|\mathbf{F}_2^l\|_{L^2(\Omega)} \leqslant C(\mathbf{u})\left(h^{k+1} + \|\boldsymbol{\xi}^{l-1}\|_{L^2(\Omega)} + \|\boldsymbol{\xi}^{l-2}\|_{L^2(\Omega)}\right); \tag{120}$$

hence for $n+1 \leqslant N$

$$\sum_{l=2}^{n+1} \Delta t \|\mathbf{F}_2^l\|_{L^2(\Omega)}^2 \leqslant C(\mathbf{u}, T)(h^{2(k+1)} + \Delta t^2 K(h, \Delta t)) + C(\mathbf{u}) \sum_{l=2}^{n} \|\boldsymbol{\xi}^l\|_{L^2(\Omega)}^2 \Delta t, \tag{121}$$

where $K(h, \Delta t)$ is the initialization error given in (72).

Proof. For any $\mathbf{x} \in \Omega$ we have from (61) and (67a)

$$\overline{\mathbf{u}}^{l-1}(\mathbf{x}) - \underline{\mathbf{u}}^{l-1}(\mathbf{x}) = \mathbf{u}^{l-1}(\overline{\mathbf{x}}) - \mathbf{u}^{l-1}(\underline{\mathbf{x}}),$$

where

$$\overline{\mathbf{x}} - \underline{\mathbf{x}} = (\mathbf{u}^{(l-1)^*} - \mathbf{U}_h^{(l-1)^*})(\mathbf{x})\Delta t.$$

Using the Taylor formula, we have

$$\begin{aligned}|(\overline{\mathbf{u}}^{l-1} - \underline{\mathbf{u}}^{l-1})(\mathbf{x})| &\leqslant \|\mathbf{u}^{l-1}\|_{W^{1,\infty}(\Omega)}\Delta t|(\mathbf{u}^{(l-1)^*} - \mathbf{U}_h^{(l-1)^*})(\mathbf{x})| \\ &\leqslant \|\mathbf{u}^{l-1}\|_{W^{1,\infty}(\Omega)}\Delta t[\leq |(\mathbf{u}^{(l-1)^*} - \mathbf{w}_h^{(l-1)^*})(\mathbf{x})| + |(\mathbf{w}_h^{(l-1)^*} - \mathbf{U}_h^{(l-1)^*})(\mathbf{x})|],\end{aligned}$$

where $\mathbf{w}_h^{(l-1)*}$ is defined as in (65a). We then obtain

$$\frac{1}{\Delta t}\|\overline{\mathbf{u}}^{l-1} - \underline{\mathbf{u}}^{l-1}\|_{L^2(\Omega)} \leqslant C(\mathbf{u})(\|\mathbf{u}^{(l-1)^*} - \mathbf{w}_h^{(l-1)^*}\|_{L^2(\Omega)} + \|\mathbf{w}_h^{(l-1)^*} - \mathbf{U}_h^{(l-1)^*}\|_{L^2(\Omega)}).$$

Using the notation (66) and the estimate (69), we have

$$\frac{1}{\Delta t}\|\overline{\mathbf{u}}^{l-1} - \underline{\mathbf{u}}^{l-1}\|_{L^2(\Omega)} \leqslant C(\mathbf{u})(h^{k+1} + \|\boldsymbol{\xi}^{l-1}\|_{L^2(\Omega)} + \|\boldsymbol{\xi}^{l-2}\|_{L^2(\Omega)}). \tag{122}$$

The estimate of $(1/\Delta t)\|\overline{\overline{\mathbf{u}}}^{l-2} - \underline{\underline{\mathbf{u}}}^{l-2}\|_{L^2(\Omega)}$ is proven in the same way and the lemma follows.

We can now introduce Lemmas 7–9.

Lemma 7

We set for $2 \leqslant l \leqslant N$

$$\mathbf{F}_3^l = \frac{3\boldsymbol{\eta}^l - 4\overline{\boldsymbol{\eta}}^{l-1} + \overline{\overline{\boldsymbol{\eta}}}^{l-2}}{2\Delta t}. \tag{123}$$

Under the hypothesis (76) we have

$$\|\mathbf{F}_3^l\|_{L^2(\Omega)} \leqslant C(\mathbf{u}, \|\mathbf{U}_h^{(l-1)^*}\|_{L^\infty(\Omega)})h^k + \frac{h^k}{\sqrt{(\Delta t)}}\left\|\frac{\partial \mathbf{u}}{\partial t}\right\|_{L^2(t^{l-2},t^l;H^k(\Omega))}; \tag{124}$$

hence for $2 \leqslant n+1 \leqslant N$

$$\sum_{l=2}^{n+1} \Delta t\|\mathbf{F}_3^l\|_{L^2(\Omega)}^2 \leqslant C(\mathbf{u}, M_n^2, T)h^{2k}, \tag{125}$$

where M_n is defined as in (78).

Proof. Let us split $\mathbf{F}_3^l$ in the form

$$\mathbf{F}_3^l = \underbrace{\frac{\frac{3}{2}(\boldsymbol{\eta}^l - \boldsymbol{\eta}^{l-1}) - \frac{1}{2}(\boldsymbol{\eta}^{l-1} - \boldsymbol{\eta}^{l-2})}{\Delta t}}_{\text{first term}=T_1} + \underbrace{\frac{2(\boldsymbol{\eta}^{l-1} - \overline{\boldsymbol{\eta}}^{l-1}) + \frac{1}{2}(\overline{\overline{\boldsymbol{\eta}}}^{l-2} - \boldsymbol{\eta}^{l-2})}{\Delta t}}_{\text{second term}=T_2}. \tag{126}$$

We have

$$\|T_1\|_{L^2(\Omega)} \leqslant \frac{3}{2}\frac{\|\boldsymbol{\eta}^l - \boldsymbol{\eta}^{l-1}\|_{L^2(\Omega)}}{\Delta t} + \frac{1}{2}\frac{\|\boldsymbol{\eta}^{l-1} - \boldsymbol{\eta}^{l-2}\|_{L^2(\Omega)}}{\Delta t}.$$

Using the definition of the norm $\|.\|_{L^2(\Omega)}$ and the Taylor formula, we get

$$\|\eta^l - \eta^{l-1}\|_{L^2(\Omega)} = \left(\int_\Omega (\eta^l(\mathbf{x}) - \eta^{l-1}(\mathbf{x}))^2 \, d\mathbf{x}\right)^{1/2}$$
$$= \left(\int_\Omega \left|\int_{t^{l-1}}^{t^l} \frac{\partial \eta}{\partial t}(\mathbf{x}, \theta) d\theta\right|^2 d\mathbf{x}\right)^{1/2}.$$

By the Cauchy–Schwarz inequality we obtain

$$\|\eta^l - \eta^{l-1}\|_{L^2(\Omega)} \leqslant \sqrt{(\Delta t)}\left(\int_\Omega \int_{t^{l-1}}^{t^l} \left|\frac{\partial \eta}{\partial t}\right|^2 (\mathbf{x}, \theta) \, d\theta \, d\mathbf{x}\right)^{1/2},$$

so that

$$\|\eta^l - \eta^{l-1}\|_{L^2(\Omega)} \leqslant \sqrt{(\Delta t)}\left\|\frac{\partial \eta}{\partial t}\right\|_{L^2((t^{l-1}, t^l); L^2(\Omega))}. \tag{127}$$

Using (69), we deduce

$$\|\eta^l - \eta^{l-1}\|_{L^2(\Omega)} \leqslant C\sqrt{(\Delta t)} h^k \left\|\frac{\partial \mathbf{u}}{\partial t}\right\|_{L^2((t^{l-1}, t^l); H^k(\Omega))}. \tag{128}$$

We estimate $\|\eta^{l-1} - \eta^{l-2}\|_{L^2(\Omega)}$ in the same way; we deduce then

$$\|T_1\|_{L^2(\Omega)} \leqslant C\frac{h^k}{\sqrt{(\Delta t)}}\left\|\frac{\partial \mathbf{u}}{\partial t}\right\|_{L^2((t^{l-2}, t^l); H^k(\Omega))}. \tag{129}$$

To handle the term T_2, we use the Taylor formula and we get from the definitions (61) and (73)

$$(\eta^{l-1} - \overline{\eta}^{l-1})(\mathbf{x}) = \eta^{l-1}(\mathbf{x}) - \eta^{l-1}(\mathbf{x} - \mathbf{U}_h^{(l-1)^*}(\mathbf{x})\Delta t)$$
$$= \eta^{l-1}(\overline{\mathbf{X}}_{\mathbf{x}}^l(t^l)) - \eta^{l-1}(\overline{\mathbf{X}}_{\mathbf{x}}^l(t^{l-1}))$$
$$= \int_{t^{l-1}}^{t^l} \frac{d}{dt}(\eta^{l-1}(\overline{\mathbf{X}}_{\mathbf{x}}^l(t))) \, dt$$
$$= \mathbf{U}_h^{(l-1)^*}(\mathbf{x}) \int_{t^{l-1}}^{t^l} \nabla \eta^{l-1}(\overline{\mathbf{X}}_{\mathbf{x}}^l(t)) \, dt.$$

Using the Cauchy–Schwarz inequality, we get

$$\|\eta^{l-1} - \overline{\eta}^{l-1}\|_{L^2(\Omega)}^2 \leqslant \Delta t \|\mathbf{U}_h^{(l-1)^*}\|_{L^\infty(\Omega)}^2 \int_\Omega \int_{t^{l-1}}^{t^l} |\nabla \eta^{l-1}(\overline{\mathbf{X}}_{\mathbf{x}}^l(t))|^2 \, dt \, d\mathbf{x}. \tag{130}$$

As Δt satisfies the condition (76), we can use in (130) the change of variables $\mathbf{y} = \overline{\mathbf{X}}_{\mathbf{x}}^l(t)$ and get according to (75)

$$\|\eta^{l-1} - \overline{\eta}^{l-1}\|_{L^2(\Omega)} \leqslant C\Delta t \|\mathbf{U}_h^{(l-1)^*}\|_{L^\infty(\Omega)} |\eta^{l-1}|_{H^1(\Omega)}. \tag{131}$$

Using similar arguments, we get

$$\|\boldsymbol{\eta}^{l-2} - \bar{\bar{\boldsymbol{\eta}}}^{l-2}\|_{L^2(\Omega)} \leqslant C\Delta t \|\mathbf{U}_h^{(l-1)^*}\|_{L^\infty(\Omega)} |\boldsymbol{\eta}^{l-2}|_{H^1(\Omega)}. \tag{132}$$

We obtain from (69), (131) and (132) the estimate

$$\|T_2\|_{L^2(\Omega)} \leqslant C(\mathbf{u}) \|\mathbf{U}_h^{(l-1)^*}\|_{L^\infty(\Omega)} h^k. \tag{133}$$

Using (126) and combining the results (129) and (133), the lemma follows.

Lemma 8

For $2 \leqslant l \leqslant N$ we set

$$\mathbf{F}_4^l = \frac{4(\bar{\boldsymbol{\xi}}^{l-1} - \boldsymbol{\xi}^{l-1}) - (\bar{\bar{\boldsymbol{\xi}}}^{l-2} - \boldsymbol{\xi}^{l-2})}{2\Delta t}. \tag{134}$$

Under the hypothesis (76) we get the estimate

$$\|\mathbf{F}_4^l\| \leqslant C(\|\mathbf{U}_h^{(l-1)^*}\|_{L^\infty(\Omega)})(|\boldsymbol{\xi}^{l-1}|_{H^1(\Omega)} + |\boldsymbol{\xi}^{l-2}|_{H^1(\Omega)}); \tag{135}$$

hence for $2 \leqslant n+1 \leqslant N$

$$\sum_{l=2}^{n+1} \Delta t \|\mathbf{F}_4^l\|_{L^2(\Omega)}^2 \leqslant C(M_n^2)\left(\sum_{l=2}^{n} \Delta t |\boldsymbol{\xi}^l|_{H^1(\Omega)}^2 + \Delta t \frac{K(h, \Delta t)}{\nu}\right). \tag{136}$$

Proof. We follow the same lines as in the analysis of the term T_2 in the second part of the previous proof until (132) with $\boldsymbol{\xi}^{l-1}$ and $\boldsymbol{\xi}^{l-2}$ instead of $\boldsymbol{\eta}^{l-1}$ and $\boldsymbol{\eta}^{l-2}$ respectively.

The following lemma states an approximation result involving the operator Π_h' defined in (54).

Lemma 9

For $2 \leqslant l \leqslant N$ we set

$$\mathbf{F}_5^l = -\nabla(\Pi_h' p^l - p^l). \tag{137}$$

We have for any $\varepsilon > 0$ and $2 \leqslant n+1 \leqslant N$

$$\left|\sum_{l=2}^{n+1} (\mathbf{F}_5^l, \boldsymbol{\xi}^l - \boldsymbol{\xi}^{l-1}\right| \leqslant \varepsilon\nu |\boldsymbol{\xi}^{n+1}|_{H^1(\Omega)}^2 + \sum_{l=2}^{n} \Delta t |\boldsymbol{\xi}^l|_{H^1(\Omega)}^2 + C\left(p, T, \frac{1}{\varepsilon\nu}\right) h^{2(k'+1)} + K(h, \Delta t). \tag{138}$$

Proof. Let us apply the Green formula and recall that $\boldsymbol{\xi}$ vanishes at the boundary; we get

$$(\mathbf{F}_5^l, \boldsymbol{\xi}^l - \boldsymbol{\xi}^{l-1}) = (\Pi_h' p^l - p^l, \nabla \cdot \boldsymbol{\xi}^l - \nabla \cdot \boldsymbol{\xi}^{l-1}). \tag{139}$$

Summing (139) from $l=2$ to $n+1$, we obtain

$$\begin{aligned}\sum_{l=2}^{n+1}(\mathbf{F}_5^l, \boldsymbol{\xi}^l - \boldsymbol{\xi}^{l-1}) &= \sum_{l=2}^{n+1}(\Pi_h' p^l - p^l, \nabla\cdot\boldsymbol{\xi}^l) - \sum_{l=1}^{n}(\Pi_h' p^{l+1} - p^{l+1}, \nabla\cdot\boldsymbol{\xi}^l)\\ &= \sum_{l=2}^{n}((\Pi_h' p - p)^l - (\Pi_h' p - p)^{l+1}, \nabla\cdot\boldsymbol{\xi}^l)\\ &\quad + (\Pi_h' p^{n+1} - p^{n+1}, \nabla\cdot\boldsymbol{\xi}^{n+1}) - (\Pi_h' p^2 - p^2, \nabla\cdot\boldsymbol{\xi}^1).\end{aligned} \tag{140}$$

Let us set $q = \Pi_h' p - p$; using the Cauchy–Schwarz inequality in (140) leads to

$$\begin{aligned}\left|\sum_{l=2}^{n+1}(\mathbf{F}_5^l, \boldsymbol{\xi}^l - \boldsymbol{\xi}^{l-1})\right| &\leqslant \sum_{l=2}^{n}\sqrt{(\Delta t)}\left\|\frac{\partial q}{\partial t}\right\|_{L^2(t^l,t^{l+1};L^2(\Omega))}|\boldsymbol{\xi}^l|_{H^1(\Omega)}\\ &\quad + \|\Pi_h' p^{n+1} - p^{n+1}\|_{L^2(\Omega)}|\boldsymbol{\xi}^{n+1}|_{H^1(\Omega)} + \|\Pi_h' p^2 - p^2\|_{L^2(\Omega)}|\boldsymbol{\xi}^1|_{H^1(\Omega)}.\end{aligned}$$

Using the inequality $2ab \leqslant a^2 + b^2$, we get for any $\varepsilon > 0$

$$\begin{aligned}\left|\sum_{l=2}^{n+1}(\mathbf{F}_5^l, \boldsymbol{\xi}^l - \boldsymbol{\xi}^{l-1})\right| &\leqslant \varepsilon\nu|\boldsymbol{\xi}^{n+1}|_{H^1(\Omega)}^2 + \sum_{l=2}^{n}\Delta t|\boldsymbol{\xi}^l|_{H^1(\Omega)}^2 + \nu|\boldsymbol{\xi}^1|_{H^1(\Omega)}^2\\ &\quad + \frac{1}{4}\left\|\frac{\partial q}{\partial t}\right\|_{L^2(0,T;L^2(\Omega))}^2 + \frac{1}{4\varepsilon\nu}\|\Pi_h' p^{n+1} - p^{n+1}\|_{L^2(\Omega)}^2\\ &\quad + \frac{C}{4\nu}\|\Pi_h' p^2 - p^2\|_{L^2(\Omega)}^2.\end{aligned} \tag{141}$$

From the initialization assumption (72), the projection error on the pressure (55) and the definition of q we deduce the result of the lemma.

From Lemmas 6–9 we can prove Lemma 5.

Proof of Lemma 5

Let us choose l, $1 \leqslant l \leqslant n$. From (60) and the definition (49) we have for any $\mathbf{v}_h$ in V_h

$$\left(\frac{3\mathbf{U}_h^{l+1} - 4\overline{\mathbf{U}}_h^l + \overline{\overline{\mathbf{U}}}_h^{l-1}}{2\Delta t}, \mathbf{v}_h\right) + \nu(\nabla\mathbf{U}_h^{l+1}, \nabla\mathbf{v}_h) - (\mathbf{f}^{l+1}, \mathbf{v}_h) = 0. \tag{142}$$

Let us subtract from (142) the quantity

$$\left(\frac{3\mathbf{w}_h^{l+1} - 4\overline{\mathbf{w}}_h^l + \overline{\overline{\mathbf{w}}}_h^{l-1}}{2\Delta t}, \mathbf{v}_h\right) + \nu(\nabla\mathbf{w}_h^{l+1}, \nabla\mathbf{v}_h);$$

we obtain with the notation (66)

$$\left(\frac{3\boldsymbol{\xi}^{l+1} - 4\overline{\boldsymbol{\xi}}^l + \overline{\overline{\boldsymbol{\xi}}}^{l-1}}{2\Delta t}, \mathbf{v}_h\right) + \nu(\nabla\boldsymbol{\xi}^{l+1}, \nabla\mathbf{v}_h) = (\mathbf{f}^{l+1}, \mathbf{v}_h) - \left(\frac{3\mathbf{w}_h^{l+1} - 4\overline{\mathbf{w}}_h^l + \overline{\overline{\mathbf{w}}}_h^{l-1}}{2\Delta t}, \mathbf{v}_h\right) - \nu(\nabla\mathbf{w}_h^{l+1}, \nabla\mathbf{v}_h).$$

From (50) and (63) we deduce that

$$\left(\frac{3\boldsymbol{\xi}^{l+1} - 4\overline{\boldsymbol{\xi}}^l + \overline{\overline{\boldsymbol{\xi}}}^{l-1}}{2\Delta t}, \mathbf{v}_h\right) + \nu(\nabla\boldsymbol{\xi}^{l+1}, \nabla\mathbf{v}_h) = (\mathbf{f}^{l+1}, \mathbf{v}_h) - \left(\frac{3\mathbf{w}_h^{l+1} - 4\overline{\mathbf{w}}_h^l + \overline{\overline{\mathbf{w}}}_h^{l-1}}{2\Delta t}, \mathbf{v}_h\right) - \nu(\nabla\mathbf{u}^{l+1}, \nabla\mathbf{v}_h),$$

which is readily transformed into

$$\begin{aligned}\left(\frac{3\xi^{l+1}-4\xi^{l}+\xi^{l-1}}{2\Delta t},\mathbf{v}_h\right)+\nu(\nabla\xi^{l+1},\nabla\mathbf{v}_h)&\\ =-\left(\frac{3\mathbf{u}^{l+1}-4\bar{\mathbf{u}}^{l}+\bar{\bar{\mathbf{u}}}_h^{l-1}}{2\Delta t}-\nu\Delta\mathbf{u}^{l+1}+\nabla p^{l+1}-\mathbf{f}^{l+1},\mathbf{v}_h\right)&\\ +(\nabla p^{l+1},\mathbf{v}_h)+\left(\frac{3\eta^{l+1}-4\bar{\eta}^{l}+\bar{\bar{\eta}}^{l-1}}{2\Delta t},\mathbf{v}_h\right)&\\ +\left(\frac{4(\bar{\xi}^{l}-\xi^{l})-(\bar{\bar{\xi}}^{l-1}-\xi^{l-1})}{2\Delta t},\mathbf{v}_h\right).&\end{aligned}\tag{143}$$

Let us introduce now the element $\Pi_h^l(p^{l+1})$ of Q_h. From the definition (49) of V_h we check that

$$\forall\mathbf{v}_h\in V_h,\quad(\Pi_h^l(p^{l+1}),\nabla\cdot\mathbf{v}_h)=0;$$

thus (143) can be rewritten as

$$\left(\frac{3\xi^{l+1}-4\xi^{l}+\xi^{l-1}}{2\Delta t},\mathbf{v}_h\right)+\nu(\nabla\xi^{l+1},\nabla\mathbf{v}_h)=\sum_{i=1}^{5}\mathbf{F}_i^{l+1}(\mathbf{v}_h),\tag{144}$$

with

$$\begin{aligned}\mathbf{F}_1^{l+1}(\mathbf{v}_h)&=-\left(\frac{3\mathbf{u}^{l+1}-4\underline{\mathbf{u}}^{l}+\underline{\underline{\mathbf{u}}}^{l-1}}{2\Delta t}-\nu\Delta\mathbf{u}^{l+1}+\nabla p^{l+1}-\mathbf{f}^{l+1},\mathbf{v}_h\right),\\ \mathbf{F}_2^{l+1}(\mathbf{v}_h)&=\left(\frac{4(\bar{\mathbf{u}}^{l}-\underline{\mathbf{u}}^{l})-(\bar{\bar{\mathbf{u}}}^{l-1}-\underline{\underline{\mathbf{u}}}^{l-1})}{2\Delta t},\mathbf{v}_h\right),\\ \mathbf{F}_3^{l+1}(\mathbf{v}_h)&=\left(\frac{3\eta^{l+1}-4\bar{\eta}^{l}+\bar{\bar{\eta}}^{l-1}}{2\Delta t},\mathbf{v}_h\right),\\ \mathbf{F}_4^{l+1}(\mathbf{v}_h)&=\left(\frac{4(\bar{\xi}^{l}-\xi^{l})-(\bar{\bar{\xi}}^{l-1}-\xi^{l-1})}{2\Delta t},\mathbf{v}_h\right),\\ \mathbf{F}_5^{l+1}(\mathbf{v}_h)&=(\Pi_h^l(p^{l+1})-p^{l+1},\nabla\cdot\mathbf{v}_h).\end{aligned}$$

For the sake of simplicity let us first set $\mathbf{F}^{l+1}=\sum_{i=1}^{5}\mathbf{F}_i^{l+1}$ and $\delta\xi^{l}=\xi^{l}-\xi^{l-1}$. Taking $\mathbf{v}_h=\delta\xi^{l+1}$ into (144), we derive

$$\begin{aligned}\frac{3}{2\Delta t}(\delta\xi^{l+1},\delta\xi^{l+1})+\nu(\nabla\xi^{l+1},\nabla\xi^{l+1})&=\frac{1}{2\Delta t}(\delta\xi^{l+1},\delta\xi^{l})\\ &+\nu(\nabla\xi^{l+1},\nabla\xi^{l})+\mathbf{F}^{l+1}(\delta\xi^{l+1}),\end{aligned}$$

which can immediately be bounded by

$$\begin{aligned}\frac{3}{2\Delta t}(\delta\xi^{l+1},\delta\xi^{l+1})+\nu(\nabla\xi^{l+1},\nabla\xi^{l+1})\leqslant\frac{1}{4\Delta t}(\delta\xi^{l},\delta\xi^{l})+\frac{1}{4\Delta t}(\delta\xi^{l+1},\delta\xi^{l+1})&\\ +\frac{\nu}{2}(\nabla\xi^{l},\nabla\xi^{l})+\frac{\nu}{2}(\nabla\xi^{l+1},\nabla\xi^{l+1})+\mathbf{F}^{l+1}(\delta\xi^{l+1});&\end{aligned}$$

thus

$$\left(\frac{5}{4\Delta t}(\delta\xi^{l+1}, \delta\xi^{l+1}) - \frac{1}{4\Delta t}(\delta\xi^{l}, \delta\xi^{l})\right) + \frac{\nu}{2}((\Delta\xi^{l+1}, \nabla\xi^{l+1}) - (\nabla\xi^{l}, \nabla\xi^{l})) \leqslant \mathbf{F}^{l+1}(\delta\xi^{l+1}). \quad (145)$$

Let us sum (145) from $l=1$ to n; we derive

$$\sum_{l=2}^{n+1} \frac{(\delta\xi^{l}, \delta\xi^{l})}{\Delta t} + \frac{\nu}{2}(\nabla\xi^{n+1}, \nabla\xi^{n+1}) \leqslant \sum_{l=2}^{n+1} \mathbf{F}^{l}(\delta\xi^{l}) + \frac{1}{4\Delta t}(\delta\xi^{1}, \delta\xi^{1}) + \frac{\nu}{2}(\nabla\xi^{1}, \nabla\xi^{1});$$

which from the initialization error (71) leads to

$$\sum_{l=2}^{n+1} \frac{(\delta\xi^{l}, \delta\xi^{l})}{\Delta t} + \frac{\nu}{2}(\nabla\xi^{n+1}, \nabla\xi^{n+1}) \leqslant \sum_{l=2}^{n+1} \mathbf{F}^{l}(\delta\xi^{l}) + K(h, \Delta t). \quad (146)$$

Using the Cauchy–Schwarz inequality and the inequality $2ab \leqslant a^2 + b^2$, it follows from (146) that

$$\frac{\nu}{2}(\nabla\xi^{n+1}, \nabla\xi^{n+1}) \leqslant C\sum_{i=1}^{4}\sum_{l=2}^{n+1} \|\mathbf{F}_i^{l}\|^2_{L^2(\Omega)}\Delta t + \left|\sum_{l=2}^{n+1} \mathbf{F}_5^{l}(\delta\xi^{l})\right| + K(h, \Delta t).$$

Then, using Lemmas 6–9, where $\varepsilon = \frac{1}{4}$ in Lemma 9, and under the condition (72) on the initialization, we obtain

$$|\xi^{n+1}|^2_{H^1(\Omega)} \leqslant \frac{C(M_n^2, \mathbf{u})}{\nu}\sum_{l=2}^{n} |\xi^{l}|^2_{H^1(\Omega)}\Delta t + C\left(\mathbf{u}, p, M_n^2, T, \frac{1}{\nu}\right)(\Delta t^4 + h^{2k} + h^{2(k'+1)}) \quad (147)$$

and (80) follows from the discrete Gronwall lemma (see Reference 25, Chap. V).

REFERENCES

1. K. Boukir, Y. Maday, A. Patera and Ronquist, 'A high order characteristics/spectral method for the incompressible Navier–Stokes equations', in preparation.
2. L. Ho, Y. Maday, A. Patera and E. Ronquist, 'A high order Lagrangian decoupling method for the incompressible Navier–Stokes equations', in C. Canuto and A. Quarteroni (eds), *Proc. ICOSAHOM '89 Meet.*, North-Holland, Amsterdam, 1990.
3. Y. Maday, A. Patera and E. Ronquist, 'An operator integration factor splitting method for time dependent problems. Application to incompressible fluid flows', *J. Sci. Comput.*, **5**, 263–292 (1990).
4. J. P. Benque, B. Ibler, A. Keramsi and G. Labadie, 'A finite element method for the Navier–Stokes equations', *Proc. Third Int. Conf. on Finite Elements in Flow Problems*, Banff, June 1980.
5. O. Pironneau, 'On the transport diffusion algorithm and its applications to the Navier–Stokes equations', *Numer. Math.*, **38**, 309–332 (1982).
6. J. Douglas and T. F. Russell, 'Numerical method for convection dominated diffusion problems based on combining the method of characteristics with finite element or finite difference procedures', *SIAM J. Numer. Anal.*, **19** (1982).
7. E. Suli, 'Convergence and nonlinear stability of the Lagrange–Galerkin method for the Navier–Stokes equations', *Numer. Math.*, **53**, 459–483 (1988).
8. E. Suli and A. Ware, 'A spectral method of characteristics for hyperbolic problems', *SIAM J. Numer. Anal.*, **28**, 423–445 (1991).
9. A. Ware, 'A spectral Lagrange–Galerkin method for convection-dominated diffusion problems', *Thesis*, 1991.
10. J. P. Chabard, 'N3S code for fluid mechanics—theoretical manual–version 3.0', *Rep. HE 41/91.30 B*, 1991.
11. R. E. Ewing and T. F. Russell, 'Multistep Galerkin method along characteristics for convection–diffusion problems', in R. Vichnevetsky and R. S. Stepleman (eds), *Advances in Computational Methods for P.D.E.*, 1981, pp. 28–36.
12. K. Boukir, B. Méetivet, E. Razafindrakoto and Y. Maday, 'Presentation of a second order time scheme using the characteristics method and applied to the Navier–Stokes equations', *Proc. IMACS '91 13th World Congr. on Computational and Applied Mathematics*, Vol. 2, Dublin, 1991, pp. 629.
13. G. C. Buscaglia and E. A. Dari, 'Implementation of the Lagrange–Galerkin method for the incompressible Navier–Stokes equations', *Int. j. numer. methods fluids*, **15**, 23–36 (1992).

14. K. Boukir, 'Méthodes en temps d'order élevé par décomposition d'opérateurs. Application aux équations de Navier–Stokes', *Thesis*, Université Pierre et Marie Curie, Mathématiques, Paris, 1993.
15. E. Suli, 'Stability and convergence of the Lagrange–Galerkin method with non-exact integration', in J. R. Whiteman (ed.), *The Mathematics of Finite Elements and Application*, Academic, New York, 1988, pp. 435–442.
16. K. W. Morton, A. Priestley and E. Suli, 'Convergence analysis of the Lagrange–Galerkin method with non-exact integration', *RAIRO M2AN*, **22**, (4), 123–151 (1988).
17. V. Girault and P. A. Raviart, *Finite Element Methods for the Navier–Stokes Equations, Theory and Algorithms*, Springer, Berlin, 1986.
18. P. G. Ciarlet, *The Finite Element Method for Elliptic Problems*, North-Holland, Amsterdam, 1978.
19. J. G. Heywood and R. Rannacher, 'Finite element approximation of the nonstationary Navier–Stokes problem. Part IV: Error analysis for the second order time discretization', *SIAM J. Numer. Anal.*, **27**, 353– 384 (1990).
20. G. Sacchi Landriani and H. Vandeven, 'Error estimates for the spectral approximation of the nonstationary Stokes problem', *SIAM J. Numer. Anal.*, **27**, 1160–1186 (1990).
21. B. Métivet, 'Résolution spectrale des equations de Navier–Stokes par une méthode de sous-domaines courbes', *Thesis*, Université Pierre et Marie Curie, Mathématiques, Paris, 1987.
22. B. Métivet and E. Razfindrakoto, 'Projet N3S de mécanique des fluides. Etude d'un schéma aux caracteristiques d'ordre 2 pour la résolution des équations de Navier–Stokes', *EDF Rep. HI72/7094*, 1990.
23. 'Numerical simulation of oscillatory convection in low-Pr fluids', in B. Roux (ed.), *Notes on Numerical Mechanics*, Vol. 27, Vieweg, Braunschweig, 1990.
24. K. Boukir, Y. Maday and B. Métivet, 'A high order characteristics method for the incompressible Navier–Stokes equations', *Comput. Methods Appl. Mech. Eng.*, **116**, 211–218 (1994).
25. V. Girault and P. A. Raviart, in A. Dold and B. Eckman (eds), *Finite Element Approximation of the Navier–Stokes Equations*, Springer, Berlin, 1981.
26. A. J. Chorin, 'Numerical solution of the Navier–Stokes equations', *Math. Comput.*, **23**, 341–353 (1969).
27. S. V. Patankar and D. B. Spalding, 'A calculation procedure for heat, mass and momentum transfer in three-dimensional parabolic flows', *Int. J. Heat Mass Transfer*, **15**, 1787–1806 (1972).
28. R. Temam, *Navier–Stokes Equations. Theory and Numerical Analysis*, North-Holland, Amsterdam, 1977.
29. J. Shen, 'On error estimates of projection methods for Navier–Stokes equations: first order scheme', *SIAM J. Numer. Anal.*, **29**, 57–77 (1992).

